

Intraspecific predator interference promotes biodiversity in ecosystems

Ju Kang^{1†}, Shijie Zhang^{2,3†}, Xin Wang^{1*}

*For correspondence:

wangxin36@mail.sysu.edu.cn (XW)

†These authors contributed equally to this work

¹School of Physics, Sun Yat-sen University, Guangzhou 510275, China; ²School of Mathematics, Sun Yat-sen University, Guangzhou 510275, China; ³Department of Mechanical Engineering, Massachusetts Institute of Technology, Cambridge, MA 02139, USA

Abstract Explaining biodiversity is a fundamental issue in ecology. A long-standing puzzle lies in the paradox of the plankton: many species of plankton feeding on a limited type of resources coexist, apparently flouting the competitive exclusion principle (CEP), which holds that the number of predator (consumer) species cannot exceed that of the resources at steady state. Here, we present a mechanistic model and show that the intraspecific interference among the consumers enables a plethora of consumer species to coexist at constant population densities with only one or a handful of resource species. The facilitated biodiversity is resistant to stochasticity, either with the stochastic simulation algorithm or individual-based modeling. Our model naturally explains the classical experiments that invalidate CEP, quantitatively illustrates the universal S-shaped pattern of the rank-abundance curves across a wide range of ecological communities, and can be broadly used to resolve the mystery of biodiversity in many natural ecosystems.

Introduction

The most prominent feature of life on Earth is its remarkable species diversity: countless macro- and micro-species fill every corner on land and in the water (*Pennisi, 2005; Hoorn et al., 2010; Vargas et al., 2015; Daniel, 2005*). In tropical forests, thousands of plant and vertebrate species coexist (*Hoorn et al., 2010*). Within a gram of soil, the number of microbial species is estimated to be 2,000-18,000 (*Daniel, 2005*). In the photic zone of the world ocean, there are roughly 150,000 eukaryotic plankton species (*Vargas et al., 2015*). Explaining the astonishing biodiversity is a major focus in ecology (*Pennisi, 2005*). A great challenge stems from the well-known competitive exclusion principle (CEP): two species competing for a single type of resources cannot coexist at constant population densities (*Gause, 1934; Hardin, 1960*), or generically, the number of consumer species cannot exceed that of resources at steady state (*MacArthur and Levins, 1964*; *McGehee and Armstrong, 1977*). On the contrary, in the paradox of plankton, a limited type of resources support hundreds or more coexisting species of phytoplankton (*Hutchinson, 1961*). Then, how can plankton and many other organisms somehow liberate the constraint of CEP?

Ever since MacArthur and Levin proposed the classical mathematical proof for CEP in the 1960s (*MacArthur and Levins, 1964*), various mechanisms have been put forward to overcome the limits set by CEP (*Chesson, 2000*). Some suggest that the system never approaches a steady state where the CEP applies, due to temporal variations (*Hutchinson, 1961; Levins, 1979*), spatial heterogeneity (*Levin, 1974*), or species' self-organized dynamics (*Koch, 1974*). Others consider factors such as toxins (*Lczárán et al., 2002*), cross-feeding (*Goyal and Maslov, 2018; Goldford et al., 2018; Niehaus et al., 2019*), spatial circulation (*Martín et al., 2020; Gupta et al., 2021*), kill the win-

ner (*Thingstad, 2000*), pack hunting (*Wang and Liu, 2020*), collective behavior (*Dalziel et al., 2021*), metabolic trade-offs (*Posfai et al., 2017; Weiner et al., 2019*), co-evolution (*Xue and Goldenfeld, 2017*), and other complex interactions among the species (*Beddington, 1975; DeAngelis et al., 1975; Arditi and Ginzburg, 1989; Kelsic et al., 2015; Grilli et al., 2017; Ratzke et al., 2020*). However, questions remain as to what determines species diversity in nature, especially for quasi-well-mixed systems such as that of the plankton (*Pennisi, 2005; Sunagawa et al., 2020*).

In this work, we present a mechanistic model of predator interference that extends the classical Beddington-DeAngelis (B-D) phenomenological model (*Beddington, 1975; DeAngelis et al., 1975*) with a detailed consideration of pairwise encounters. The intraspecific interference among consumer individuals effectively constitutes a negative feedback loop, enabling a wide range of consumer species to coexist with only one or a few types of resources. The coexistence state is resistant to stochasticity and can hence be realized in practice. Our model is broadly applicable and can be used to explain biodiversity in many ecosystems. In particular, it naturally explains species coexistence in classical experiments that invalidate CEP (*Ayala, 1969*), and quantitatively illustrates the S-shaped pattern of the rank-abundance curves in an extensive spectrum of ecological communities, ranging from the communities of ocean plankton worldwide (*Fuhrman et al., 2008*), tropical river fishes from Argentina (*Cody et al., 1996*), forest bats of Trinidad (*Clarke et al., 2005*), rainforest trees (*Hubbell, 2001*), birds (*Terborgh et al., 1990*), butterflies (*Devries et al., 1997*) in Amazonia, to those of desert bees (*Hubbell, 2001*) in Utah and lizards from South Australia (*Cody et al., 1996*).

Results

A generic model of pairwise encounter

Predator interference, i.e., the pairwise encounter among consumer individuals, is commonly described by the B-D model (*Beddington, 1975; DeAngelis et al., 1975*). From the mechanistic perspective, however, the functional response of the B-D model can be formally derived from the consumption between a consumer species and a resource species without involving any form of predator interference (*Wang and Liu, 2020; Huisman and Boer, 1997*) (see Appendix II B). To resolve this issue, we consider a mechanistic model of pairwise encounters (Fig. 1A). Specifically, S_C consumer species $\{C_1, \dots, C_{S_C}\}$ competing for S_R resource species $\{R_1, \dots, R_{S_R}\}$. The consumers are biotic, while the resources can be either biotic or abiotic. For simplicity, we assume that all species are motile and each moves at a certain speed, namely, v_{C_i} for consumer species C_i ($i = 1, \dots, S_C$) and v_{R_l} for resource species R_l ($l = 1, \dots, S_R$). For abiotic resources, they cannot propel themselves, yet may passively drift due to environmental factors. Each consumer is free to feast on one or multiple types of resources, while consumers do not directly interact with one another other than pairwise encounters.

Then, we proceed to explicitly consider the population structure of the consumers and resources: some are wandering around freely, taking Brownian motions; others are encountering with one another, forming ephemeral entangled pairs. Specifically, when a consumer individual C_i and a resource R_l get close in space within a distance of $r_{il}^{(C)}$ (Fig. 1A), the consumer can chase the resource and form a chasing pair: $C_i^{(P)} \vee R_l^{(P)}$ (Fig. 1B), where the superscript "(P)" represents pair. The resource can either escape with rate d_{il} or be caught and consumed by the consumer with rate k_{il} . Meanwhile, when a C_i individual encounters another consumer C_j ($j = 1, \dots, S_C$) of the same or different species within a distance of $r_{ij}^{(C)}$ (Fig. 1A), they can stare at, fight against or play with each other and thus form an interference pair: $C_i^{(P)} \vee C_j^{(P)}$ (Fig. 1B). This paired state is evanescent, and the two consumers separate from each other with rate d'_{ij} . For simplicity, we assume that all $r_{il}^{(C)}$ and $r_{ij}^{(C)}$ are identical, respectively, i.e., $\forall i, j, l, r_{il}^{(C)} = r^{(C)}$ and $r_{ij}^{(C)} = r^{(C)}$.

In a well-mixed system with the size of L^2 (Appendix-fig. 1), the encounter rates among the species, a_{il} and a'_{ij} (Fig. 1B), can be obtained using the mean-field approximation: $a_{il} = 2r^{(C)}L^{-2}\sqrt{v_{C_i}^2 + v_{R_l}^2}$ and $a'_{ij} = 2r^{(C)}L^{-2}\sqrt{v_{C_i}^2 + v_{C_j}^2}$ (see Materials and Methods, and Appendix-fig. 1 for details). Then, we

proceed to analyze scenarios involving different types of pairwise encounters. For the scenario involving only chasing pair, the population dynamics can be described as follows:

$$\begin{cases} \dot{x}_{il} = a_{il}C_i^{(F)}R_l^{(F)} - (d_{il} + k_{il})x_{il}, \\ \dot{C}_i = \sum_{l=1}^{S_R} w_{il}k_{il}x_{il} - D_iC_i, \quad i = 1, \dots, S_C, \\ \dot{R}_l = g_l(\{R_l\}, \{x_i\}, \{C_i\}), \quad l = 1, \dots, S_R, \end{cases} \quad (1)$$

where $x_{il} \equiv C_i^{(P)} \vee R_l^{(P)}$, g_l is an unspecified function, the superscript "(F)" represents the freely wandering population, D_i denotes the mortality rate of C_i , and w_{il} is the mass conversion ratio (, **Wang and Liu, 2020**) from resource R_l to consumer C_i . With the integration of intraspecific predator interference, we combine Eq. 1 and the following equation:

$$\dot{y}_i = a'_i[C_i^{(F)}]^2 - d'_iy_i, \quad (2)$$

where $a'_i = a'_{ii}$, $d'_i = d'_{ii}$, and $y_i \equiv C_i^{(P)} \vee C_i^{(P)}$ represents the intraspecific interference pair. For the scenario involving chasing pair and interspecific interference, we combine Eq. 1 with the following equation:

$$\dot{z}_{ij} = a'_{ij}C_i^{(F)}C_j^{(F)} - d'_{ij}z_{ij}, \quad i \neq j, \quad (3)$$

where $z_{ij} \equiv C_i^{(P)} \vee C_j^{(P)}$ stands for the interspecific interference pair. In the scenario where chasing pair and both intra- and inter-specific interference are all relevant, we combine Eqs. 1-3, and the populations of consumers and resources are given by $C_i = C_i^{(F)} + \sum_l x_{il} + 2y_i + \sum_{j \neq i} z_{ij}$ and $R_l = R_l^{(F)} + \sum_i x_{il}$, respectively.

Generically, the consumption and interference processes are much quicker compared to the birth and death processes. Thus, in derivation of the functional response, $\mathcal{F}(R_l, C_i) \equiv k_{il}x_{il}/C_i$, the consumption and interference processes are supposed to be in fast equilibrium. In all scenarios involving different types of pairwise encounters, the functional response in the B-D model is a good approximation only for a special case with $d_{il} \approx 0$ and $R_l \gg \sum_{i=1}^{S_C} C_i$ (Appendix-fig. 2, see Appendix II for details).

To facilitate further analysis, we assume that the population dynamics of the resources follows the same construction rule as that in MacArthur's consumer-resource model (, **MacArthur, 1970; Chesson, 1990**). Then,

$$g_l(\{R_l\}, \{x_i\}, \{C_i\}) = \begin{cases} R_0^{(l)}R_l(1 - R_l/K_0^{(l)}) - \sum_{i=1}^{S_C} k_{il}x_{il} & \text{(for biotic resources);} \\ R_a^{(l)}(1 - R_l/K_0^{(l)}) - \sum_{i=1}^{S_C} k_{il}x_{il} & \text{(for abiotic resources).} \end{cases} \quad (4)$$

In the absence of consumers, biotic resources exhibit logistic growth. Here, $R_0^{(l)}$ and $K_0^{(l)}$ represent the intrinsic growth rate and the carrying capacity of species R_l . For abiotic resources, $R_a^{(l)}$ stands for the external resource supply rate of R_l , and $K_0^{(l)}$ is the abundance of R_l at steady state without consumers. For simplicity, we focus our analysis on abiotic resources, although all results generally apply to biotic resources as well. By applying dimensional analysis, we render all parameters dimensionless (see Appendix VI). For convenience, we retain the same notations below, with all parameters considered dimensionless unless otherwise specified.

Intraspecific predator interference facilitates species coexistence and breaks CEP

To clarify the specific mechanisms that can facilitate species coexistence, we systematically investigate scenarios involving different forms of pairwise encounters in a simple case with $S_C = 2$ and $S_R = 1$. To simplify the notations, we omit the subscript/superscript "l" since $S_R = 1$. For clarity, we assign each consumer species of unique competitiveness by setting that the mortality rate D_i is the only parameter that varies with the consumer species.

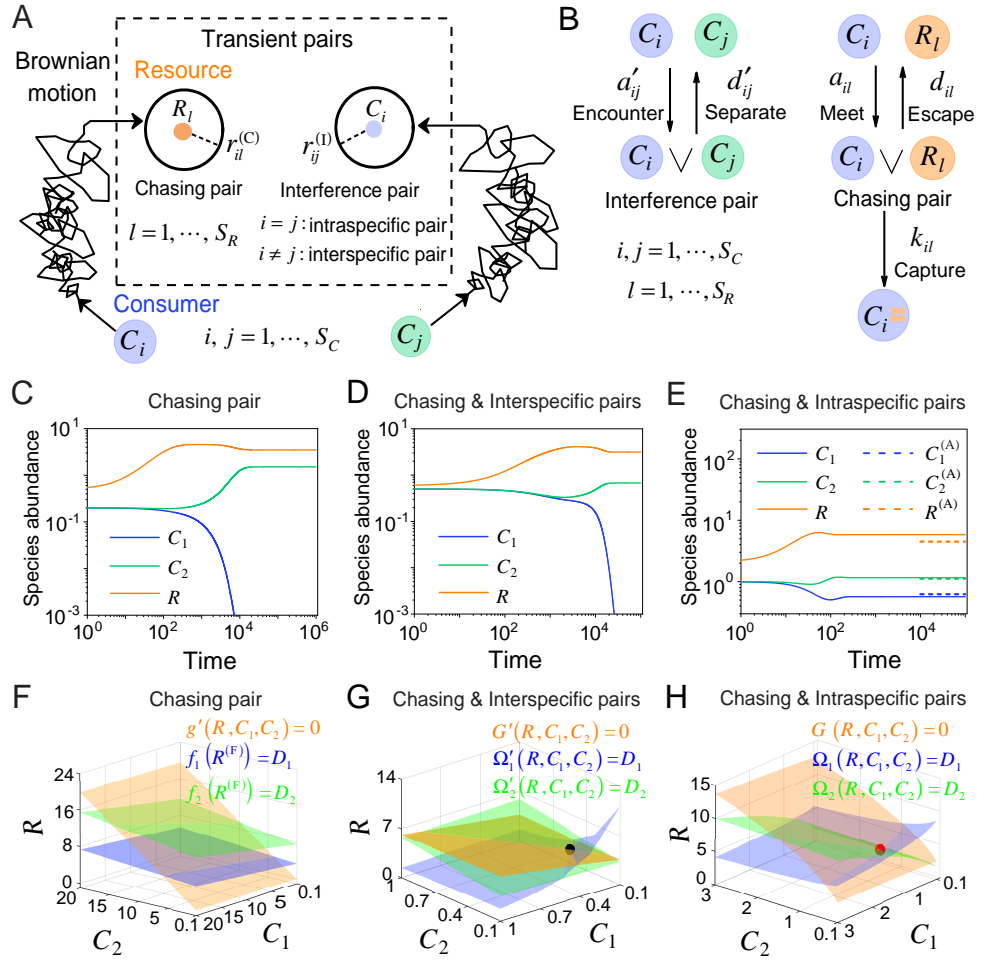


Figure 1. A model of pairwise encounters may naturally break CEP. (A) A generic model of S_C consumer species feeding on S_R resource species with pairwise encounters. (B) The well-mixed model of (A). (C-E) Time courses of two consumer species competing for one resource species. (F-H) Positive solutions to the steady-state equations: $\dot{R} = 0$ (orange surface), $\dot{C}_1 = 0$ (blue surface), $\dot{C}_2 = 0$ (green surface). The black/red dot represents the unstable/stable fixed point, while the dotted lines in (E) are the analytical solutions of the steady-state abundances (marked with superscript "(A)"). See Appendix VII for simulation details.

First, we conduct the analysis in a deterministic framework with ordinary differential equations (ODEs). In the scenario involving only chasing pair, consumer species cannot coexist at steady state except for special parameter settings (sets of measure zero) (Wang and Liu, 2020). In practice, if all species coexist, the steady-state equations of the consumer species ($\dot{C}_i = 0$) yield $f_i(R^{(F)}) \equiv R^{(F)}/(R^{(F)} + K_i) = D_i$ ($i = 1, 2$), with $K_i = (d_i + k_i)/a_i$, which corresponds to two parallel surfaces in the (C_1, C_2, R) coordinates, making steady coexistence impossible (Wang and Liu, 2020) (Fig. 1C, F).

Meanwhile, in the scenario involving chasing pair and interspecific interference, if all species coexist, the steady-state equations correspond to three non-parallel surfaces $\Omega'_i(R, C_1, C_2) = D_i$ ($i = 1, 2$), $G'(R, C_1, C_2) = 0$ (Fig. 1G and Appendix-fig. 3C, see Appendix IV for details), which can intersect at a common point (fixed point). However, this fixed point is unstable (Fig. 1G, Appendix-fig. 3A), and thus one of the consumer species is doom to extinct (Fig. 1D).

Next, we turn to the scenario involving chasing pair and intraspecific interference. Likewise, steady coexistence requires that three non-parallel surfaces $\Omega_i(R, C_1, C_2) = D_i$ ($i = 1, 2$), $G(R, C_1, C_2) = 0$ (Fig. 1H and Appendix-fig. 3D, see Appendix III for details) cross at a common point. Indeed, this naturally happens, and encouragingly the fixed point can be stable. Therefore, two consumer species may stably coexist at steady state with only one type of resources, which obviously breaks

CEP (Fig. 1E Appendix-fig. 4A). In fact, the coexisting state is globally attractive (Appendix-fig. 4A), and there exists a non-zero volume of parameter space where the two consumer species stably coexist at constant population densities (Appendix-fig. 4B), demonstrating that the violation of CEP does not depend on special parameter settings. We further consider the scenario involving chasing pair and both intra- and inter-specific interference (Appendix-fig. 5). Much as expected, the species coexistence behavior is very similar to that without interspecific interference.

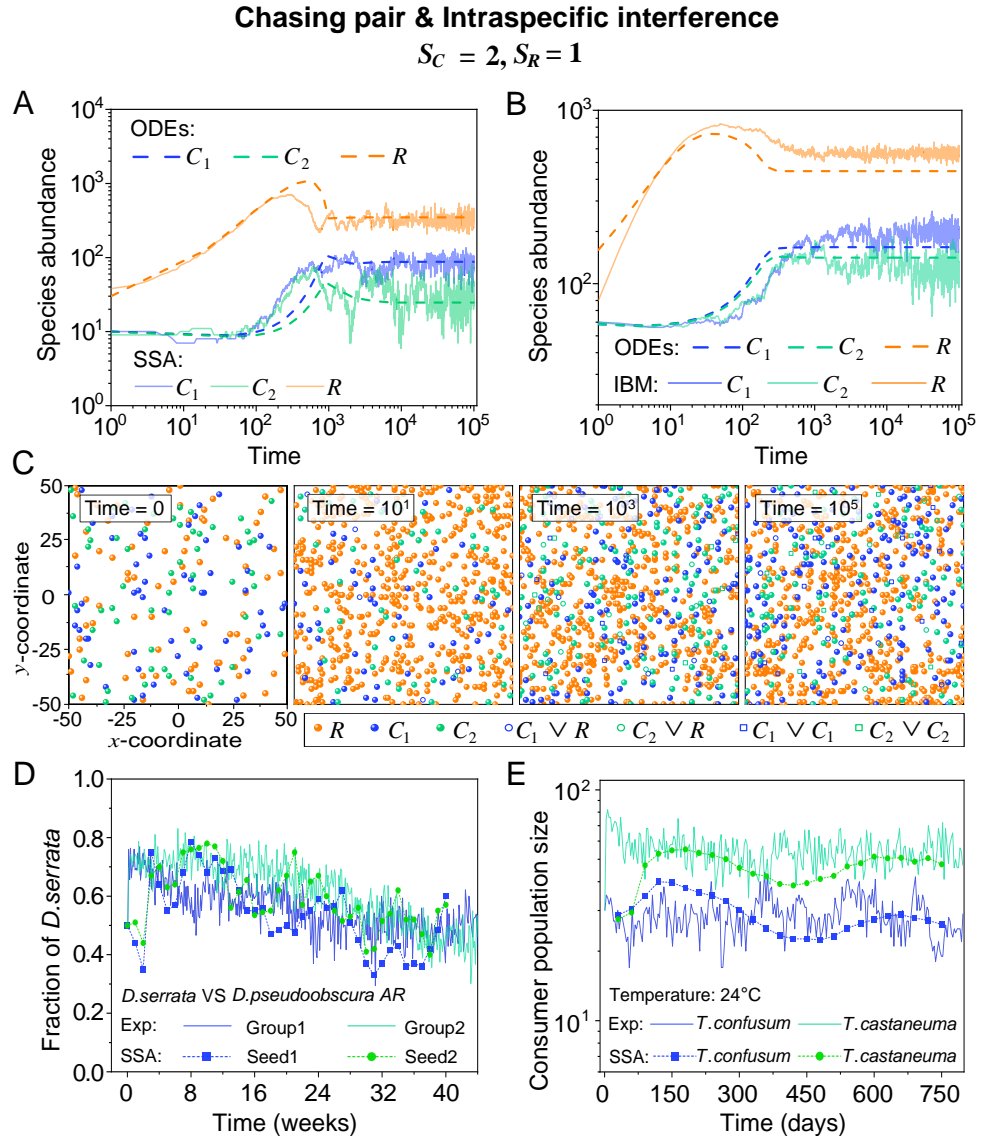


Figure 2. Intraspecific predator interference facilitates species coexistence regardless of stochasticity. (A-B) Time courses of the species abundances simulated with ODEs, SSA, or IBM. (C) Snapshots of the IBM simulations. (D-E) A model of intraspecific predator interference explains two classical laboratory experiments that invalidate CEP. (D) In Ayala's experiment, two *Drosophila* species coexist with one type of resources within a laboratory bottle (, *Ayala, 1969*). (E) In Park's experiment, two *Tribolium* species coexist for two years with one type of food (flour) within a lab (, *Park, 1954*).

Intraspecific interference promotes biodiversity in the presence of stochasticity

Stochasticity is ubiquitous in nature. However, it is prone to jeopardize species coexistence (*Xue and Goldenfeld, 2017*). Influential mechanisms such as "kill the winner" fail when stochasticity is incorporated (*Xue and Goldenfeld, 2017*). Consistent with this, we observe that two notable

cases of oscillating coexistence (, Koch, 1974,H) turn into species extinction when stochasticity is introduced (Appendix-fig. 6A-B), where we simulate the models with stochastic simulation algorithm (SSA) (Gillespie, 2007) and adopt the same parameters as those in the original references (, Koch, 1974,H).

Then, we proceed to investigate the impact of stochasticity on our model using SSA (Gillespie, 2007). In the scenario involving chasing pair and intraspecific interference, species may coexist indefinitely in the SSA simulations (Fig. 2A and Appendix-fig. 4C). In fact, the parameter region for species coexistence in this scenario is rather similar between the SSA and ODEs studies (Appendix-fig. 6C-D). Similarly, in the scenario involving chasing pair and both inter- and intra-specific interference, all species may coexist indefinitely in company with stochasticity (Appendix-fig. 5D).

To further mimic a real ecosystem, we resort to individual-based modeling (IBM) (Grimm and Railsback, 2013; Vetsigian, 2017), an essentially stochastic simulation method. In the simple case of $S_C = 2$ and $S_R = 1$, we simulate the time evolution of a 2-D squared system in a size of L^2 with periodic boundary conditions (see Materials and Methods for details). In the scenario involving chasing pair and intraspecific interference, two consumer species coexist for long with only one type of resources in the IBM simulations (Fig. 2B-C). Together with the SSA simulation studies, it is obvious that intraspecific interference promotes species coexistence along with stochasticity.

Comparison with experimental studies that reject CEP

In practice, two classical studies (, Ayala, 1969,P) reported that, in their respective laboratory systems, two species of insects coexisted for roughly years or more with only one type of resources. Evidently, these two experiments (, Ayala, 1969,P) are incompatible with CEP, while factors such as temporal variations, spatial heterogeneity, cross-feeding, etc. are clearly not involved in such systems. As intraspecific fighting is prevalent among insects (Boomsma et al., 2005; Dankert et al., 2009; Chen et al., 2002), we apply the model involving chasing pair and intraspecific interference to simulate the two systems. Overall, our SSA results show good consistency with those of the experiments (Fig. 2D-E, see also Appendix-figs. 6C-D, 7). The fluctuations in experimental time series can be mainly accounted by stochasticity.

A handful of resource species can support an unexpected wide range of consumer species regardless of stochasticity

To resolve the puzzle stated in the paradox of the plankton, we analyze the generic case where S_C consumers species compete for S_R resource species (with $S_C > S_R$) within the scenario involving chasing pair and intraspecific interference. The population dynamics is described by equations combining Eqs. 1, 2, 4. As with the cases above, each consumer species is assigned a unique competitiveness through a distinctive D_i ($i = 1, \dots, S_C$).

Strikingly, a plethora of consumer species may coexist at steady state with only one resource species ($S_C \gg S_R$, $S_R = 1$) in the ODEs simulations, and crucially, the facilitated biodiversity can still be maintained in the SSA simulations. The long-term coexistence behavior are exemplified in Fig. 3 and Appendix-fig. 8-10, involving simulations with or without stochasticity. The number of consumer species in long-term coexistence can be up to hundreds or more (Fig. 3 and Appendix-fig. 8). To mimic the real ecosystems, we further analyze the cases with more than one type of resources, such as systems with $S_R = 3$ ($S_C \gg S_R$). Just like the case of $S_R = 1$ ($S_C \gg S_R$), an extensive range of consumer species may coexist indefinitely regardless of stochasticity (Fig. 3 and Appendix-fig. 11-14).

Intuitive understanding: an underlying negative feedback loop

For the case with only one resource species ($S_R = 1$), if the total population size of the resources is much larger than that of the consumers (i.e., $R \gg \sum_{i=1}^{S_C} C_i$), the functional response $F \equiv k_i x_i / C_i$ and the steady-state population of each consumer and resource species can be obtained analytically

(see Appendix III B-C for details). In fact, the functional response of a consumer species (e.g., C_i) is negatively correlated with its own population size:

$$F(R, C_i) \approx \frac{2R}{\sqrt{(R + K_i)^2 + 8\beta_i K_i^2 C_i + R + K_i}}, \quad (5)$$

where $\beta_i \equiv a'_i/d'_i$. The analytical steady-state solutions are highly consistent with the numerical results (Fig. 1E and Appendix-fig. 3E-F) and can even quantitatively predict the coexistence region of the parameter space (Appendix-fig. 3F).

Intuitively, the mechanisms of how intraspecific interference facilitates species coexistence can be understood from the underlying negative feedback loop. Specifically, for consumer species of higher competitiveness (e.g., C_i) in an ecological community, as the population size of C_i increases during competition, a larger portion of C_i individuals are then engaged in intraspecific interference pairs which are temporarily absent from hunting (see Eq. S59 and Appendix-fig. 15A-B). Consequently, the fraction of C_i individuals within chasing pairs decreases (see Eq. S59 and Appendix-fig. 15A-B) and thus form a self-inhibiting negative feedback loop through the functional response (see Eq. S59 and Appendix-fig. 15C). This negative feedback loop prevents further increases in C_i populations, results in an overall balance among the consumer species, and thus promotes biodiversity (see Appendix III C for details).

The S shape pattern of the rank-abundance curves in a broad range of ecological communities

As mentioned above, a prominent feature of biodiversity is that the species' rank-abundance curves follow a universal S-shaped pattern in the linear-log plot across a broad spectrum of ecological communities (, *Fuhrman et al., 2008*, S,C,T,M,C,H; *Devries et al., 1997*). Previously, this pattern was mostly explained by the neutral theory (, *Hubbell, 2001*), which requires special parameter settings that all consumer species share identical fitness. To resolve this issue, we apply the model involving chasing pair and intraspecific interference to simulate the ecological communities, where one or three types of resources support a large number of consumer species ($S_C \gg S_R$). In each model system, the mortality rates of consumer species follow a Gaussian distribution where the coefficient of variation was taken round 0.3 (, *Menon et al., 2003*) (see Appendix VII for details). For a broad array of the ecological communities, the rank-abundance curves obtained from the long-term coexisting state of both the ODEs and SSA simulation studies agree quantitatively with those of experiments (Fig. 3C-D, see also Appendix-figs. 8-14), sharing roughly equal Shannon entropies and mostly being regarded as identical distributions in the Kolmogorov-Smirnov (K-S) statistical test (with a significance threshold of 0.05). Still, there is a noticeable discrepancy between the experimental data and SSA studies in terms of the species' absolute abundances (e.g., Appendix-fig. 8C): those with experimental abundances less than 10 tend to extinct in the SSA simulations. This is due to the fact that the recorded individuals in an experimental sample are just a tiny portion of that in the real ecological system, whereas the species population size in a natural community is certainly much larger than 10.

Discussion

The conflict between the CEP and biodiversity, exemplified by the paradox of the plankton (*Hutchinson, 1961*), is a long-standing puzzle in ecology. Although many mechanisms have been proposed to overcome the limit set by CEP (*Hutchinson, 1961; Chesson, 2000; Levins, 1979; Levin, 1974; Koch, 1974,H; Lczárán et al., 2002; Goyal and Maslov, 2018; Goldford et al., 2018; Martín et al., 2020; Gupta et al., 2021; Thingstad, 2000; Wang and Liu, 2020; Dalziel et al., 2021; Posfai et al., 2017; Weiner et al., 2019; Xue and Goldenfeld, 2017; Beddington, 1975; DeAngelis et al., 1975; Arditi and Ginzburg, 1989; Kelsic et al., 2015; Grilli et al., 2017; Ratzke et al., 2020*), it is still unclear how plankton and many other organisms can flout CEP and maintain biodiversity in quasi-well-mixed natural ecosystems. To address this issue, we investigate a mechanistic model with

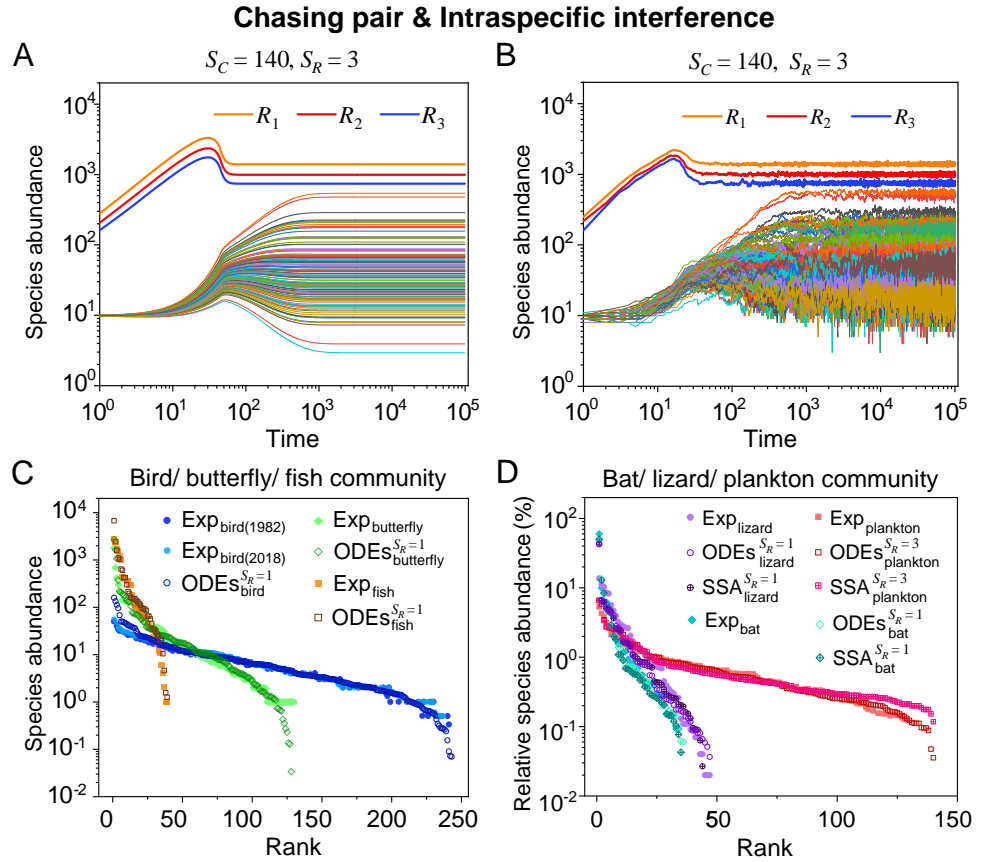


Figure 3. Intraspecific interference enables a wide range of consumer species to coexist with only one or a handful of resource species. (A-B) Representative time courses simulated with ODEs and SSA. (C-D) A model of intraspecific predator interference illustrates the S-shaped pattern of the species' rank-abundance curves across different ecological communities. The solid icons represent the experimental data (marked with "Exp") reported in existing studies (, [Fuhrman et al., 2008](#), C,T,M,C; [Devries et al., 1997](#); , [Hubbell, 2001](#)) where the bird community data were collected longitudinally in 1982 and 2018 (, [Terborgh et al., 1990](#), M). The ODEs and SSA results were constructed from timestamp $t = 1.0 \times 10^5$ in the time series. In the K-S test, the probabilities (p values) that the simulation results and the corresponding experimental data come from the same distributions are: $p_{\text{ODEs}}^{\text{bird}(1982)} = 0.17$, $p_{\text{ODEs}}^{\text{bird}(2018)} = 0.26$, $p_{\text{ODEs}}^{\text{butterfly}} = 0.70$, $p_{\text{ODEs}}^{\text{fish}} = 0.88$; $p_{\text{ODEs}}^{\text{bat}} = 0.42$, $p_{\text{SSA}}^{\text{bat}} = 0.48$, $p_{\text{ODEs}}^{\text{lizard}} = 0.96$, $p_{\text{SSA}}^{\text{lizard}} = 0.54$; $p_{\text{ODEs}}^{\text{plankton}} = 0.20$, $p_{\text{SSA}}^{\text{plankton}} = 0.06$. See Appendix VII for simulation details and the Shannon entropies.

detailed consideration of pairwise encounters. Using numerical simulations combined with mathematical analysis, we identify that the intraspecific interference among the consumer individuals can promote a wide range of consumer species to coexist indefinitely with only one or a handful of resource species through the underlying negative feedback loop. By applying the above analysis to real ecological systems, our model naturally explains two classical experiments that reject CEP (, [Ayala, 1969](#), P), and quantitatively illustrates the universal S-shaped pattern of the rank-abundance curves for a broad range of ecological communities (, [Fuhrman et al., 2008](#), S,C,T,M,C,H; [Devries et al., 1997](#)).

In fact, predator interference has been introduced long ago by the B-D model (, [Beddington, 1975](#); [DeAngelis et al., 1975](#)). However, the functional response of the B-D model involving intraspecific interference can be formally derived from the scenario involving only chasing pair without predator interference (, [Wang and Liu, 2020](#); [Huisman and Boer, 1997](#)) (see Eqs. S8 and S24). Therefore, it is questionable regarding the validity of applying the B-D model to break CEP. From mechanistic perspective, we resolve these issues and show that B-D model corresponds to a special case of our mechanistic model yet without the escape rate (Appendix-fig. 2, see Appendix II for details).

Our model is broadly applicable to explain biodiversity in many ecosystems. In practice, many more factors are potentially involved, and special attention is required to disentangle confounding factors. In microbial systems, complex interactions are commonly involved (Goyal and Maslov, 2018; Goldford et al., 2018; Hu et al., 2022), and species' preference for food is shaped by the evolution course and environmental history (Wang et al., 2019). It is still highly challenging to fully explain how organisms evolve and maintain biodiversity in diverse ecosystems.

Methods and Materials

Derivation of the encounter rates with the mean-field approximation

In the model depicted in Fig. 1A, consumers and resources move randomly in space, which can be regarded as Brownian motions. At moment t , a consumer individual of species C_i ($i = 1, \dots, S_C$) moves at speed v_{C_i} with velocity $\mathbf{v}_{C_i}(t)$, while a resource individual of species R_l ($l = 1, \dots, S_R$) moves at speed v_{R_l} with velocity $\mathbf{v}_{R_l}(t)$. Here v_{C_i} and v_{R_l} are two invariants, while the directions of $\mathbf{v}_{C_i}(t)$ and $\mathbf{v}_{R_l}(t)$ change constantly. The relative velocity between the two individuals is $\mathbf{u}_{C_i-R_l}(t) \equiv \mathbf{v}_{R_l}(t) - \mathbf{v}_{C_i}(t)$, with a relative speed of $u_{C_i-R_l}(t)$. Then, $u_{C_i-R_l}(t)^2 = v_{C_i}^2 + v_{R_l}^2 - 2v_{C_i} \cdot v_{R_l} \cdot \cos \theta_{C_i-R_l}(t)$, where $\theta_{C_i-R_l}(t)$ represents the angle between $\mathbf{v}_{C_i}(t)$ and $\mathbf{v}_{R_l}(t)$. This system is homogeneous, thus, $\overline{\cos \theta_{C_i-R_l}} = 0$, where the overline stands for the temporal average. Then, we obtain the average relative speed between the C_i and R_l individuals: $\overline{u_{C_i-R_l}} = \sqrt{v_{C_i}^2 + v_{R_l}^2}$. Likewise, the average relative speed between the C_i and C_j individuals is $\overline{u_{C_i-C_j}} = \sqrt{v_{C_i}^2 + v_{C_j}^2}$. Evidently, $\overline{u_{C_i-C_i}} = \sqrt{2}v_{C_i}$. Meanwhile, the concentrations of species C_i and R_l in a squared system with a length of L are $n_{C_i} = C_i/L^2$ and $n_{R_l} = R_l/L^2$, while those of the freely wandering C_i and R_l are $n_{C_i}^{(F)} = C_i^{(F)}/L^2$ and $n_{R_l}^{(F)} = R_l^{(F)}/L^2$.

Then, we use the mean-field approximation to calculate the encounter rates a_{il} and a'_{ij} in the well-mixed system. In particular, we estimate a_{il} by tracking a randomly chosen consumer individual from species C_i and counting its encounter frequency with the freely wandering individuals from resource species R_l (Appendix-fig. 1). At any moment, the consumer individual may form a chasing pair with a R_l individual within a radius of $r_{il}^{(C)}$ (Fig. 1A). Over a time interval of Δt , the number of encounters between the consumer individual and R_l individuals can be estimated by the encounter area and the concentration n_{R_l} , which takes the value of $2r_{il}^{(C)} n_{R_l} \overline{u_{C_i-R_l}} \Delta t$ (see Appendix-fig. 1). Combined with $n_{R_l}^{(F)} = R_l^{(F)}/L^2$, for all freely wandering C_i individuals, the number of their encounters with $R_l^{(F)}$ during interval Δt is $\frac{2r_{il}^{(C)} \overline{u_{C_i-R_l}} C_i^{(F)} R_l^{(F)}}{L^2} \Delta t$. Meanwhile, in the ODEs, this corresponds to $a_i C_i^{(F)} R_l^{(F)} \Delta t$. Comparing both terms above, for chasing pair, we have $a_{il} = 2r_{il}^{(C)} L^{-2} \overline{u_{C_i-R_l}} = 2r_{il}^{(C)} L^{-2} \sqrt{v_{C_i}^2 + v_{R_l}^2}$. Likewise, for interference pair, we obtain $a'_{ij} = 2r_{ij}^{(I)} L^{-2} \overline{u_{C_i-C_j}} = 2r_{ij}^{(I)} L^{-2} \sqrt{v_{C_i}^2 + v_{C_j}^2}$. In particular, $a'_{ii} = 2\sqrt{2}v_{C_i} r_{ii}^{(I)} L^{-2}$.

Stochastic simulations

To investigate the impact of stochasticity on species coexistence, we use stochastic simulation algorithm (SSA) (Gillespie, 2007) and individual-based modeling (IBM) (Vetsigian, 2017; Grimm and Railsback, 2013) in simulating the stochastic process. In the SSA studies, we follow the standard Gillespie algorithm and simulation procedures (Gillespie, 2007).

In the IBM studies, we consider a 2D squared system in a length of L with periodic boundary conditions. In the case of $S_C = 2$ and $S_R = 1$, consumers of species C_i ($i = 1, 2$) move at speed v_{C_i} , while the resources move at speed v_R . The unit length is $\Delta l = 1$, while all individuals move probabilistically. Specifically, when Δt is small so that $v_{C_i} \Delta t \ll 1$, C_i individuals jump a unit length with the probability $v_{C_i} \Delta t$. In practice, we simulate the temporal evolution of the model system following the procedures below.

Initialization. We choose the initial position for each individual randomly from a uniform distribution in the squared space, which round to the nearest integer point in the x - y coordinates.

Moving. We choose the destination of a movement randomly from four directions (x -positive, x -negative, y -positive, y -negative) following a uniform distribution. The consumers and resources

jump a unit length with probabilities $v_{C_i}\Delta t$ and $v_R\Delta t$, respectively.

Forming pairs. When a C_i individual and a resource individual get close in space within a distance of $r^{(C)}$, they form a chasing pair. Meanwhile, when two consumer individuals C_i and C_j stand within a distance of $r^{(I)}$, they form an interference pair.

Dissociation. We update the system with a small time step Δt so that $d_i\Delta t, k_i\Delta t, d'_{ij}\Delta t \ll 1$ ($i, j = 1, 2$). In practice, a random number ζ is sampled from a uniform distribution between 0 and 1, i.e., $\mathcal{U}(0, 1)$. If $\zeta < d_i\Delta t$ or $\zeta < d'_{ij}\Delta t$, then, the chasing pair or interference pair dissociates into two separated individuals. One occupies the original position, while the other individual gets just out of the encounter radius in a uniformly distributed random angle. For a chasing pair, if $d_i\Delta t < \zeta < (d_i + k_i)\Delta t$, then, the consumer catch the resource, and the biomass of the resource flows into the consumer populations (updated according to the birth procedure), while the consumer individual occupies the original position. Finally, if $\zeta > (d_i + k_i)\Delta t$ or $\zeta > d'_{ij}\Delta t$, the chasing pair or interference pair maintain the current status.

Birth and death. For each species, we use two separate counters with decimal precision to record the contributions of the birth and death processes, which both accumulate in each time step. The incremental integer part of the counter will trigger updates in this run. Specifically, a newborn would join the system following the initialization procedure in a birth action, while an unfortunate target would be randomly chosen from the living population in a death action.

Author contributions

X.W. conceived and designed the project; J.K., S.Z. and X. W. performed research; J.K. and X. W. analyzed data and wrote the paper.

Competing interests

The authors declares no competing interests.

Data and materials availability

All study data are included in the article and/or appendices.

Acknowledgments

We thank Roy Kishony, Eric D. Kelsic, Yang-Yu Liu and Fan Zhong for helpful discussions. This work was supported by National Natural Science Foundation of China (Grant No.12004443), Guangzhou Municipal Innovation Fund (Grant No.202102020284) and the Hundred Talents Program of Sun Yat-sen University.

References

- Arditi R, Ginzburg LR. Coupling in predator-prey dynamics: ratio-dependence. *Journal of Theoretical Biology.* 1989; 139(3):311-326. doi: [https://doi.org/10.1016/S0022-5193\(89\)80211-5](https://doi.org/10.1016/S0022-5193(89)80211-5).
- Ayala FJ. Experimental invalidation of the principle of competitive exclusion. *Nature.* 1969; 224:1076-1079. doi: <https://doi.org/10.1038/2241076a0>.
- Beddington JR. Mutual interference between parasites or predators and its effect on searching efficiency. *Journal of Animal Ecology.* 1975; 44(1):331-340. doi: <https://doi.org/10.2307/3866>.
- Boomsma JJ, Baer B, Heinze J. The evolution of male traits in social insects. *Annual Review of Entomology.* 2005; 50:395-420. doi: <https://doi.org/10.1146/annurev.ento.50.071803.130416>.
- Chen S, Lee AY, Bowens NM, Huber R, Kravitz EA. Fighting fruit flies: a model system for the study of aggression. *PNAS.* 2002; 99(8):5664-5668. doi: <https://doi.org/10.1073/pnas.082102599>.
- Chesson P. Macarthur's consumer-resource model. *Journal of Theoretical Biology.* 1990; 37(1):26-38. doi: [https://doi.org/10.1016/0040-5809\(90\)90025-Q](https://doi.org/10.1016/0040-5809(90)90025-Q).

- Chesson P.** Mechanisms of maintenance of species diversity. *Annual Review of Ecology and Systematics*. 2000; 31:343–336. doi: <https://www.jstor.org/stable/221736>.
- Clarke FM, Rostant LV, Racey PA.** Life after logging: post-logging recovery of a neotropical bat community. *Journal of Applied Ecology*. 2005; 42:409–420. doi: <https://doi.org/10.1111/j.1365-2664.2005.01024.x>.
- Cody ML, Smallwood JA.** *Long-Term Studies of Vertebrate Communities*. Academic Press. 1996.
- Dalziel BD, Novak M, Watson JR, Ellner SP.** Collective behaviour can stabilize ecosystems. *Nature Ecology & Evolution*. 2021; 5:1435–1440. doi: <https://doi.org/10.1038/s41559-021-01517-w>.
- Daniel R.** The metagenomics of soil. *Nature Reviews Microbiology*. 2005; 3:470–478. doi: <http://dx.doi.org/10.1038/nrmicro1160>.
- Dankert H, Wang L, Hoopfer ED, Anderson DJ, Perona P.** Automated monitoring and analysis of social behavior in drosophila. *Nature Methods*. 2009; 6:297–303. doi: <https://doi.org/10.1038/nmeth.1310>.
- DeAngelis DL, Goldstein RA, O'Neill RV.** A model for trophic interaction. *Ecology*. 1975; 56(4):881–892. doi: <https://doi.org/10.2307/1936298>.
- Devries PJ, Murray D, Lande R.** Species diversity in vertical, horizontal, and temporal dimensions of a fruit-feeding butterfly community in an ecuadorian rainforest. *Biological Journal of the Linnean Society*. 1997; 62(3):343–364. doi: <https://doi.org/10.1006/bjil.1997.0155>.
- Fuhrman JA, Steele JA, Hewson I, Schwalbach MS, Brown MV, Green JL, Brown JH.** A latitudinal diversity gradient in planktonic marine bacteria. *PNAS*. 2008; 105:7774–7778. doi: <https://doi.org/10.1073/pnas.0803070105>.
- Gause GF.** *The Struggle for Existence*. The Williams & Wilkins Company, Baltimore 1934.
- Gillespie DT.** Stochastic simulation of chemical kinetics. *Annual Review of Physical Chemistry*. 2007; 58:35–55. doi: <https://doi.org/10.1146/annurev.physchem.58.032806.104637>.
- Goyal A, Lu N, Bajić D, Estrela S, Tikhonov M, Sanchez-Gorostiaga A, Segrè D, Mehta P, Sanchezvz A.** Emergent simplicity in microbial community assembly. *Science*. 2018; 361:469–474. doi: <https://doi.org/10.1126/science.aat1168>.
- Goyal A, Maslov S.** Diversity, stability, and reproducibility in stochastically assembled microbial ecosystems. *Physical Review Letters*. 2018; 120:158102. doi: <https://doi.org/10.1103/PhysRevLett.120.158102>.
- Grilli J, Barabás G, Michalska-Smith MJ, Allesina S.** Higher-order interactions stabilize dynamics in competitive network models. *Nature*. 2017; 548:210–213. doi: <https://doi.org/10.1038/nature23273>.
- Grimm V, Railsback SF.** *Individual-based Modeling and Ecology*. Princeton University Press. 2013.
- Gupta D, Garlaschi S, Suweis S, Azae S, Maritan A.** Effective resource competition model for species coexistence. *Physical Review Letters*. 2021; 127:208101. doi: <https://doi.org/10.1103/PhysRevLett.127.208101>.
- Hardin G.** The competitive exclusion principle. *Science*. 1960; 131(3049):1292–1297. doi: <http://dx.doi.org/10.1126/science.131.3409.1292>.
- Hoorn C, Wesselingh FP, ter Steege H, Bermudez MA, Mora A, Sevink J, Sanmartín I, Sanchez-Meseguer A, Anderson CL, Figueiredo JP, Jaramillo C, Riff D, Negri FR, Hooghiemstra H, Lundberg J, Stadler T, Särkinen T, Antonelli A.** Amazonia through time: Andean uplift, climate change, landscape evolution, and biodiversity. *Science*. 2010; 330:927–931. doi: <http://dx.doi.org/10.1126/science.1194585>.
- Hu J, Amor DR, Barbier M, Bunin G, Gore J.** Emergent phases of ecological diversity and dynamics mapped in microcosms. *Science*. 2022; 378(6615):85–89. doi: <https://doi.org/10.1126/science.abm7841>.
- Hubbell SP.** *The Unified Neutral Theory of Biodiversity and Biogeography*. Princeton University Press. 2001.
- Huisman G, Boer RJD.** A formal derivation of the "beddington" functional response. *Journal of Theoretical Biology*. 1997; 185(3):389–400. doi: <https://doi.org/10.1006/jtbi.1996.0318>.
- Huisman J, Weissing FJ.** Biodiversity of plankton by species oscillations and chaos. *Nature*. 1999; 402:407–410. doi: <https://doi.org/10.1038/46540>.
- Hutchinson GE.** The paradox of the plankton. *The American Naturalist*. 1961; 95:137–145. doi: <http://dx.doi.org/10.1086/282171>.

- Kelsic ED**, Zhao J, Vetsigian K, Kishony R. Counteraction of antibiotic production and degradation stabilizes microbial communities. *Nature*. 2015; 521:516–519. doi: <https://doi.org/10.1038/nature14485>.
- Koch AL**. Competitive coexistence of two predators utilizing the same prey under constant environmental conditions. *Journal of Theoretical Biology*. 1974; 44(2):387–395. doi: [https://doi.org/10.1016/0022-5193\(74\)90169-6](https://doi.org/10.1016/0022-5193(74)90169-6).
- Lczárán T**, Hoekstra RF, Pagie L. Chemical warfare between microbes promotes biodiversity. *PNAS*. 2002; 99:786–790. doi: <https://doi.org/10.1073/pnas.012399899>.
- Levin SA**. Community equilibria and stability, and an extension of the competitive exclusion principle. *The American Naturalist*. 1970; 104(939):413–423. doi: <https://www.jstor.org/stable/2459310>.
- Levin SA**. Dispersion and population interactions. *The American Naturalist*. 1974; 108:207–228. doi: <https://doi.org/10.1086/282900>.
- Levins R**. Coexistence in a variable environment. *The American Naturalist*. 1979; 114:765–783. doi: <https://doi.org/10.1086/283527>.
- MacArthur R**. Species packing and competitive equilibrium for many species. *Journal of Theoretical Biology*. 1970; 1(1):1–11. doi: [https://doi.org/10.1016/0040-5809\(70\)90039-0](https://doi.org/10.1016/0040-5809(70)90039-0).
- MacArthur R**, Levins R. Competition, habitat selection, and character displacement in a patchy environment. *PNAS*. 1964; 51:1207–1210. doi: <http://dx.doi.org/10.1073/pnas.51.6.1207>.
- Martín PV**, Buček A, Bourguignon T, Pigolotti S. Ocean currents promote rare species diversity in protists. *Science Advances*. 2020; 6:eaaz9037. doi: <https://doi.org/10.1126/sciadv.aaz9037>.
- Martínez AE**, Ponciano JM, Gomez JP, Valqui T, Novoa J, Antezana M, Biscarra G, Camerlenghi E, Carnes BH, Munarriz RH, Parra E, Plummer IM, Fitzpatrick JW, Robinson SK, Socolar JB, Terborgh J. The structure and organisation of an Amazonian bird community remains little changed after nearly four decades in Manu National Park. *Ecology Letters*. 2023; 26(2):335–34. doi: <https://doi.org/10.1111/ele.14159>.
- McGehee R**, Armstrong RA. Some mathematical problems concerning the ecological principle of competitive exclusion. *Journal of Differential Equations*. 1977; 23(1):30–52. doi: [http://dx.doi.org/10.1016/0022-0396\(77\)90135-8](http://dx.doi.org/10.1016/0022-0396(77)90135-8).
- Menon P**, Billen G, Servais P. Mortality rates of autochthonous and fecal bacteria in natural aquatic ecosystems. *Water Research*. 2003; 37(17):4151–4158. doi: [https://doi.org/10.1016/S0043-1354\(03\)00349-X](https://doi.org/10.1016/S0043-1354(03)00349-X).
- Niehaus L**, Boland I, Liu M, Chen K, Fu D, Henckel C, Chaung K, Miranda SE, Dyckman S, Crum M, Dedrick S, Shou W, Momeni B. Microbial coexistence through chemical-mediated interactions. *Nature Communications*. 2019; 10:2052–474. doi: <https://doi.org/10.1038/s41467-019-10062-x>.
- Park T**. Experimental studies of interspecies competition ii. temperature, humidity, and competition in two species of tribolium. *Physiological Zoology*. 1954; 27:177–238. doi: <https://doi.org/10.1086/physzool.27.3.30152164>.
- Pennisi E**. What determines species diversity? *Science*. 2005; 309:90–90. doi: <http://dx.doi.org/10.1126/science.309.5731.9>.
- Posfai A**, Taillefumier T, Wingreen NS. Metabolic trade-offs promote diversity in a model ecosystem. *Physical Review Letters*. 2017; 118:028103. doi: <https://doi.org/10.1103/PhysRevLett.118.028103>.
- Ratzke C**, Barrere J, Gore J. Strength of species interactions determines biodiversity and stability in microbial communities. *Nature Ecology & Evolution*. 2020; 4:376–383. doi: <https://doi.org/10.1038/s41559-020-1099-4>.
- Ser-Giacomi E**, Zinger L, Malviya S, Vargas CD, Karsenti E, Bowler C, Monte SD. Ubiquitous abundance distribution of non-dominant plankton across the global ocean. *Nature Ecology & Evolution*. 2018; 2:1243–1249. doi: <https://doi.org/10.1038/s41559-018-0587-2>.
- Sunagawa S**, Acinas SG, Bork P, Bowler C, Coordinators TO, Eveillard D, Gorsky G, Guidi L, Iudicone D, Karsenti E, Lombard F, Ogata H, Pesant S, Sullivan MB, Wincker P, Vargas CD. Tara oceans: towards global ocean ecosystems biology. *Nature Reviews Microbiology*. 2020; 18:428–445. doi: <https://doi.org/10.1038/s41579-020-0364-5>.

- Terborgh J**, Robinson SK, Parker III TA, Munn CA, Pierpont N. Structure and organization of an amazonian forest bird community. *Ecological Monographs*. 1990; 60(2):213–238. doi: <https://doi.org/10.2307/1943045>.
- Thingstad TF**. Elements of a theory for the mechanisms controlling abundance, diversity, and biogeochemical role of lytic bacterial viruses in aquatic systems. *Limnology and Oceanography*. 2000; 45:1320–1328. doi: <https://doi.org/10.4319/lo.2000.45.6.1320>.
- Vargas CD**, Audic S, Henry N, Decelle J, Mahé F, Logares R, Lara E, Berney C, Bescot NL, Probert I, Carmichael M, Poulain J, Romac S, Colin S, Aury JM, Bittner L, Chaffron S, Dunthorn M, Engelen S, Flegontova O, Guidi L, Horák A, Jaillon O, Lima-Mendez G, Lukeš J, Malviya S, Morard R, Mulot M, Scalco E, Siano R, Vincent F, Zingone A, Dimier C, Picheral M, Searson S, Kandels-Lewis S, Coordinators TO, Acinas SG, Bork P, Bowler C, Gorsky G, Grimsley N, Hingamp P, Iudicone D, Not F, Ogata H, Pesant S, Raes J, Sieracki ME, Speich S, Stemmann L, Sunagawa S, Weissenbach J, Wincker P, Karsenti E. Eukaryotic plankton diversity in the sunlit ocean. *Science*. 2015; 348:1261605. doi: <http://dx.doi.org/10.1126/science.1261605>.
- Vetsigian K**. Diverse modes of eco-evolutionary dynamics in communities of antibiotic producing microorganisms. *Nature Ecology & Evolution*. 2017; 1:0189. doi: <https://doi.org/10.1038/s41559-017-0189>.
- Wang X**, Liu YY. Overcome competitive exclusion in ecosystems. *iScience*. 2020; 23:101009. doi: <https://doi.org/10.1016/j.isci.2020.101009>.
- Wang X**, Xia K, Yang X, Tang C. Growth strategy of microbes on mixed carbon sources. *Nature Communications*. 2019; 10:1279. doi: <https://doi.org/10.1038/s41467-019-09261-3>.
- Weiner BG**, Posfai A, Wingreen NS. Spatial ecology of territorial populations. *PNAS*. 2019; 116:17874–17879. doi: <https://doi.org/10.1073/pnas.1911570116>.
- Xue C**, Goldenfeld N. Coevolution maintains diversity in the stochastic "kill the winner" model. *Physical Review Letters*. 2017; 119:268101. doi: <https://doi.org/10.1103/PhysRevLett.119.268101>.

Appendices for Intraspecific predator interference promotes biodiversity in ecosystems

Appendix I The classical proof of Competitive Exclusion Principle (CEP)

In the 1960s, MacArthur (*MacArthur and Levins, 1964*) and Levin (*Levin, 1970*) put forward the classical mathematical proof of CEP. We rephrase their idea in the simple case of $S_C = 2$ and $S_R = 1$, i.e., two consumer species C_1 and C_2 competing for one resource species R . In practice, this proof can be generalized into higher dimensions with several consumer and resource species. The population dynamics of the system can be described as follows:

$$\begin{cases} \dot{C}_i = C_i(f_i(R) - D_i), & i = 1, 2; \\ \dot{R} = g(R, C_1, C_2). \end{cases} \quad (S1)$$

Here C_i and R represent the population abundances of consumers and resources, respectively, while the functional forms of $f_i(R)$ and $g(R, C_1, C_2)$ are unspecific. D_i stands for the mortality rate of the species C_i . If all consumer species can coexist at steady state, then $f_i(R)/D_i = 1$ ($i = 1, 2$). In a 2-D representation, this requires that three lines $y = f_i(R)/D_i$ ($i = 1, 2$) and $y = 1$ share a common point, which is commonly impossible unless the model parameters satisfy special constraint (sets of Lebesgue measure zero). In a 3-D representation, the two planes corresponding to $f_i(R)/D_i = 1$ ($i = 1, 2$) are parallel, and hence do not share a common point (see Ref. (*Wang and Liu, 2020*) for details).

Appendix II Comparison of the functional response with Beddington-DeAngelis (B-D) model

A B-D model

In 1975, Beddington proposed a mathematical model (*Beddington, 1975*) to describe the influence of predator interference on the functional response with hand-waving derivations. In the same year, DeAngelis and his colleagues considered a related question and put forward a similar model (*DeAngelis et al., 1975*). Essentially, both models are phenomenological, and they were called B-D model in the subsequent studies. In practice, the B-D model can be extended into scenarios involving different types of pairwise encounters with Beddington's modelling method. In this section, we systematically compare the functional response in B-D model with that of our mechanistic model in all the relevant scenarios.

Recalling Beddington's analysis, the model (*Beddington, 1975*) consists of one consumer species C and one resource species R ($S_C = 1, S_R = 1$). In a well-mixed system, an individual consumer meets a resource with rate a , while encounters another consumer with rate a' . There are two other phenomenological parameters in this model, namely, the handling time t_h and the wasting time t_w . Both can be determined by specifying the scenario and using statistical physics modeling analysis. In fact, Beddington analyzed the searching efficiency Ξ_{B-D} rather than the functional response F_{B-D} , yet both can be reciprocally derived with $\Xi_{B-D} \equiv F_{B-D}/R$. Here R stands for the population abundance of the resources, and the specific form of Ξ_{B-D} is (*Beddington, 1975*):

$$\Xi_{B-D}(R, C) = \frac{a}{1 + at_h R + a't_w C'}, \quad (S2)$$

where $C' = C - 1$, and C stands for the population abundance of the consumes. Generally, $C \gg 1$, and thus $C' \approx C$.

B Scenario involving only chasing pair

Here we consider the scenario involving only chasing pair for the simple case with one consumer species C and one resource species R ($S_C = 1, S_R = 1$). When an individual consumer is chasing a resource, they form a chasing pair:

$$C^{(F)} + R^{(F)} \xrightleftharpoons[d]{a} C^{(P)} \vee R^{(P)} \xrightarrow{k} C^{(F)(+)},$$

where the superscript “(F)” stands for populations that are freely wandering, and “(+)” signifies gaining biomass (we count $C^{(F)(+)}$ as $C^{(F)}$). $C^{(P)} \vee R^{(P)}$ represents chasing pair (where “(P)” signifies pair), denoted as x . a , d and k stand for encounter rate, escape rate and capture rate, respectively. Hence, the total number of consumers and resources are $C \equiv C^{(F)} + x$ and $R \equiv R^{(F)} + x$. Then, the population dynamics of the system follows:

$$\begin{cases} \dot{x} = aC^{(F)}R^{(F)} - (k+d)x, \\ \dot{C} = w k x - DC, \\ \dot{R} = g(R, x, C). \end{cases} \quad (S3)$$

Here the functional form of $g(R, x, C)$ is unspecific, while D and w represent the mortality rate of the consumer species and biomass conversion ratio (Wang and Liu, 2020), respectively. Since consumption process is generically much faster than the birth/death process, in deriving the functional response, the consumption process is supposed to be in fast equilibrium (i.e., $\dot{x} = 0$). Then, we can solve for x with:

$$x^2 - (R + C + K)x + RC = 0, \quad (S4)$$

where $K = \frac{k+d}{a}$, and then,

$$x = \frac{2RC}{(R + C + K)} \frac{1}{\left(1 + \sqrt{1 - \frac{4RC}{(R+C+K)^2}}\right)}. \quad (S5)$$

By definition, the functional response and search efficiency are:

$$F_{CP}(R, C) = \frac{kx}{C}, \quad (S6a)$$

$$\Xi_{CP}(R, C) = \frac{kx}{RC}. \quad (S6b)$$

Hence, we obtain the functional response and search efficiency in this chasing-pair scenario:

$$F_{CP}(R, C)_{(1)} = k \frac{(R + C + K)}{2C} \left(1 - \sqrt{1 - \frac{4RC}{(R + C + K)^2}}\right), \quad (S7a)$$

$$\Xi_{CP}(R, C)_{(1)} = k \frac{(R + C + K)}{2RC} \left(1 - \sqrt{1 - \frac{4RC}{(R + C + K)^2}}\right). \quad (S7b)$$

Since $\frac{4RC}{(R+C+K)^2} < 4\frac{C}{R} \ll 1$, using first order approximations in Eq. S7, we obtain $\sqrt{1 - \frac{4RC}{(R+C+K)^2}} \approx 1 - \frac{2RC}{(R+C+K)^2}$. Then the functional response and search efficiency are:

$$F_{CP}(R, C)_{(2)} = k \frac{R}{R + C + K}, \quad (S8a)$$

$$\Xi_{CP}(R, C)_{(2)} = \frac{k}{R + C + K}. \quad (S8b)$$

Evidently, there is no predator interference within the chasing-pair scenario, yet the functional response form is identical to the B-D model involving intraspecific interference (see Eq. S2). Meanwhile, using first order approximations in the denominator of Eq. S5, we have $x \approx \frac{RC}{(R+C+K) - \frac{RC}{(R+C+K)}}$. Hence,

$$F_{CP}(R, C)_{(3)} = k \frac{R}{(R + C + K) - \frac{RC}{(R+C+K)}}, \quad (S9a)$$

$$\Xi_{CP}(R, C)_{(3)} = \frac{k}{(R + C + K) - \frac{RC}{(R+C+K)}}. \quad (S9b)$$

In the case that $R \gg C$, then $R \gg C > x = R - R^{(F)}$. By applying $R \approx R^{(F)}$ in Eq. S3, we obtain $x \approx \frac{RC}{R+K}$. Then,

$$\mathcal{F}_{\text{CP}}(R, C)_{(4)} = k \frac{R}{R+K}, \quad (\text{S10a})$$

$$\Xi_{\text{CP}}(R, C)_{(4)} = \frac{k}{R+K}. \quad (\text{S10b})$$

To compare these functional responses with that of the B-D model, we determine the parameters t_h and t_w in the B-D model by calculating their ensemble average values in a stochastic framework. Using the properties of waiting time distribution in the Poisson process, we obtain $\langle t_h \rangle = \frac{1}{k}$ and $\langle t_w \rangle = \frac{1}{a'}$ (in the chasing-pair scenario, $a' = 0$). By substituting these calculations into Eq. S2, we have

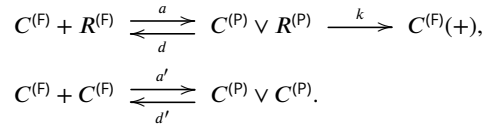
$$\Xi_{\text{CP}}^{\text{B-D}}(R, C) = \frac{a}{1 + Ra/k} = \frac{k}{k/a + R}, \quad (\text{S11a})$$

$$\mathcal{F}_{\text{CP}}^{\text{B-D}}(R, C) = \frac{kR}{k/a + R}. \quad (\text{S11b})$$

In the special case with $d = 0$ and $R \gg C$, the B-D model is consistent with our mechanistic model: $\Xi_{\text{B-D}}(R, C) = \Xi_{\text{CP}}(R, C)_{(4)}$. Outside the special region, however, the discrepancy can be considerably large (see Appendix-fig. 2A-B for the comparison).

C Scenario involving chasing pair and intraspecific interference

Here we consider the scenario with additional involvement of intraspecific interference in the simple case of $S_C = 1$ and $S_R = 1$



Here $C^{(P)} \vee C^{(P)}$ stands for the intraspecific predator interference pair, denoted as y ; a' and d' represent the encounter rate and separation rate of the interference pair, respectively. Then, the total population of consumers and resources are $C \equiv C^{(F)} + x + 2y$ and $R \equiv R^{(F)} + x$. Hence the population dynamics of the consumers and resources can be described as follows:

$$\begin{cases} \dot{x} = aC^{(F)}R^{(F)} - (k+d)x, \\ \dot{y} = a'[C^{(F)}]^2 - d'y, \\ \dot{C} = wkx - DC, \\ \dot{R} = g(R, x, C). \end{cases} \quad (\text{S12})$$

The consumption process and interference process are supposed to be in fast equilibrium (i.e., $\dot{x} = 0, \dot{y} = 0$), then we can solve for x with:

$$x^3 + \phi_2 x^2 + \phi_1 x + \phi_0 = 0, \quad (\text{S13})$$

where $\phi_0 = -CR^2$, $\phi_1 = 2CR + KR + R^2$, $\phi_2 = 2\beta K^2 - K - C - 2R$, with $\beta = a'/d'$. The discriminant of Eq. S13 (denoted as Λ) is

$$\Lambda = -4\psi^3 - 27\varphi^2, \quad (\text{S14})$$

with $\psi = \phi_1 - (\phi_2)^2/3$ and $\varphi = \phi_0 - \phi_1\phi_2/3 + 2(\phi_2)^3/27$. When $\Lambda < 0$, there are one real solution $x_{(1)}$ and two complex solutions $x_{(2)}, x_{(3)}$, which are

$$x_{(1)} = \theta_1 + \theta_2 - \phi_2/3, x_{(2)} = \omega\theta_1 + \omega^2\theta_2 - \phi_2/3, x_{(3)} = \omega^2\theta_1 + \omega\theta_2 - \phi_2/3, \quad (\text{S15})$$

where $\omega = -1/2 + i\sqrt{3}/2$ (i stands for the imaginary unit), $\theta_1 = (-\varphi/2 + \sqrt{-\Lambda/108})^{1/3}$, and $\theta_2 = (-\varphi/2 - \sqrt{-\Lambda/108})^{1/3}$. On the other hand, when $\Lambda > 0$, there are three real solutions $x_{(1)}$, $x_{(2)}$, and $x_{(3)}$, which are

$$x_{(1)} = \psi' \cos \varphi' - \phi_2/3, x_{(2)} = \psi' \cos(\varphi' + \frac{2\pi}{3}) - \phi_2/3, x_{(3)} = \psi' \cos(\varphi' + \frac{4\pi}{3}) - \phi_2/3, \quad (S16)$$

where $\psi' = (-4\psi/3)^{1/2}$ and $\varphi' = \arccos(-(-\psi/3)^{-3/2}\varphi/2)/3$. Note that $x \in [0, \min(R, C)]$, then we obtain the exact feasible solution of x (denoted as x_{ext}), and hence the functional response and search efficiency are

$$\mathcal{F}_{\text{intra}}(R, C)_{(1)} = \frac{kx_{\text{ext}}}{C}, \quad (S17a)$$

$$\Xi_{\text{intra}}(R, C)_{(1)} = \frac{kx_{\text{ext}}}{RC}. \quad (S17b)$$

In the case of $R \gg C$, then $R - R^{(F)} = x < C \ll R$, and thus $R^{(F)} \approx R$. Still, the consumption process is supposed to be in fast equilibrium (i.e., $\dot{x} = 0, \dot{y} = 0$), and then we obtain

$$x \approx \frac{RC}{\sqrt{[\frac{1}{2}(K+R)]^2 + 2C\beta K^2} + \frac{1}{2}(K+R)}. \quad (S18)$$

Consequently,

$$\mathcal{F}_{\text{intra}}(R, C)_{(2)} = k \frac{R}{\sqrt{[\frac{1}{2}(K+R)]^2 + 2C\beta K^2} + \frac{1}{2}(K+R)}, \quad (S19a)$$

$$\Xi_{\text{intra}}(R, C)_{(2)} = k \frac{1}{\sqrt{[\frac{1}{2}(K+R)]^2 + 2C\beta K^2} + \frac{1}{2}(K+R)}. \quad (S19b)$$

When $\beta \ll \frac{1}{8C}$ or $8\beta C/(1+R/K)^2 \ll 1$, using first order approximations in the denominator of Eq. S18, we have

$$x \approx \frac{RC}{(K+R) + \frac{2K}{(1+R/K)}\beta C}, \quad (S20)$$

and then,

$$\mathcal{F}_{\text{intra}}(R, C)_{(3)} = k \frac{R}{(K+R) + \frac{2K}{(1+R/K)}\beta C}, \quad (S21a)$$

$$\Xi_{\text{intra}}(R, C)_{(3)} = k \frac{1}{(K+R) + \frac{2K}{(1+R/K)}\beta C}. \quad (S21b)$$

In the case that $8\beta C/(1+R/K)^2 \gg 1$, using first order approximations in Eq. S18, we obtain

$$x \approx \frac{RC}{K\sqrt{2C\beta} + \frac{(K+R)^2}{8K\sqrt{2C\beta}} + \frac{1}{2}(K+R)}, \quad (S22)$$

and thus,

$$\mathcal{F}_{\text{intra}}(R, C)_{(4)} = k \frac{R}{K\sqrt{2C\beta} + \frac{(K+R)^2}{8K\sqrt{2C\beta}} + \frac{1}{2}(K+R)}, \quad (S23a)$$

$$\Xi_{\text{intra}}(R, C)_{(4)} = k \frac{1}{K\sqrt{2C\beta} + \frac{(K+R)^2}{8K\sqrt{2C\beta}} + \frac{1}{2}(K+R)}. \quad (S23b)$$

Meanwhile, the B-D model only fits to the cases with $d = 0$. By calculating the average values of t_h and t_w in the stochastic framework, we have $\langle t_h \rangle = \frac{1}{k}$, $\langle t_w \rangle = \frac{1}{d'}$. Thus, we obtain the searching efficiency and functional response in the B-D model:

$$\Xi_{\text{intra}}^{\text{B-D}}(R, C) = \frac{a}{1 + \frac{a}{k}R + \frac{a}{d'}C} = \frac{a}{1 + R/K|_{d=0} + \beta C}, \quad (S24a)$$

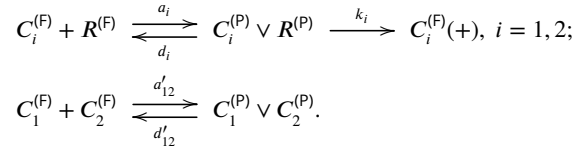
$$\mathcal{F}_{\text{intra}}^{\text{B-D}}(R, C) = \frac{aR}{1 + R/K|_{d=0} + \beta C}. \quad (S24b)$$

Overall, the searching efficiency (and the functional response) of the B-D model is quite different from either the rigorous form $\Xi_{\text{intra}}(R, C)_{(1)}$, the quasi rigorous form $\Xi_{\text{intra}}(R, C)_{(2)}$, or the more simplified forms $\Xi_{\text{intra}}(R, C)_{(3)}$ and $\Xi_{\text{intra}}(R, C)_{(4)}$ (Appendix-fig. 2C-D). Still, there is a region where the discrepancies can be small, namely $d \approx 0$ and $R \gg C$ (Appendix-fig. 2C-D). Intuitively, when $\beta \ll \frac{1}{8C}$ and $d = 0$, then $\Xi_{\text{intra}}(R, C)_{(3)} = \frac{a}{1 + \frac{a}{k}R + \frac{a^2}{(1+R/K)\beta C_i}}$. Consequently, if $R/K_i = x/C_i^{(F)} < 1$, then $\frac{2}{(1+R/K_i)} \in [1, 2]$. In this case, the difference between $\Xi_{\text{intra}}^{\text{B-D}}(R, C)$ and $\Xi_{\text{intra}}(R, C)_{(3)}$ is small.

In fact, the above analysis also applies to cases with more than one types of consumer species (i.e., for cases with $S_C > 1$).

D Scenario involving chasing pair and interspecific interference

Next, we consider the scenario involving chasing pair and interspecific interference in the case of $S_C = 2$ and $S_R = 1$:



Here $C_1^{(P)} \vee C_2^{(P)}$ stands for the interspecific interference pair, denoted as z ; a'_{12} and d'_{12} represent the encounter rate and separation rate of the interference pair, respectively. Then, the total population of consumers and resources are $C_i \equiv C_i^{(F)} + x_i + z$ and $R \equiv R^{(F)} + x_1 + x_2$. The population dynamics of the consumers and resources follows:

$$\begin{cases} \dot{x}_i = a_i C_i^{(F)} R^{(F)} - (k_i + d_i)x_i, \quad i = 1, 2; \\ \dot{z} = a'_{12} C_1^{(F)} C_2^{(F)} - d'_{12} z, \\ \dot{C}_i = w_i k_i x_i - D_i C_i, \\ \dot{R} = g(R, x_1, x_2, C_1, C_2). \end{cases} \quad (\text{S25})$$

where the functional form of $g(R, x_1, x_2, C_1, C_2)$ is unspecific, while D_i and w_i represents the mortality rates of the two consumers species and biomass conversion ratios. Still, the consumption/interference process is supposed to be in fast equilibrium, i.e., $\dot{x}_i = 0, \dot{z} = 0$. In the case that $R \gg C_1 + C_2 > x_1 + x_2$, by applying $R^{(F)} \approx R$, we obtain

$$x_1 \approx \frac{2C_1(R/K_2 + 1)R/K_1}{\sqrt{[\gamma(C_2 - C_1) + (\frac{R}{K_1} + 1)(\frac{R}{K_2} + 1)]^2 + 4\gamma C_1(\frac{R}{K_1} + 1)(\frac{R}{K_2} + 1) + \gamma(C_2 - C_1) + (\frac{R}{K_1} + 1)(\frac{R}{K_2} + 1)}}, \quad (\text{S26a})$$

$$x_2 \approx \frac{2C_2(R/K_1 + 1)R/K_2}{\sqrt{[\gamma(C_1 - C_2) + (\frac{R}{K_1} + 1)(\frac{R}{K_2} + 1)]^2 + 4\gamma C_2(\frac{R}{K_1} + 1)(\frac{R}{K_2} + 1) + \gamma(C_1 - C_2) + (\frac{R}{K_1} + 1)(\frac{R}{K_2} + 1)}}. \quad (\text{S26b})$$

Then, the searching efficiencies and functional responses are:

$$\Xi_1^{\text{inter}}(RC_1, C_2)_0 = \frac{2k_1(R/K_2 + 1)/K_1}{\gamma(C_2 - C_1) + (\frac{R}{K_1} + 1)(\frac{R}{K_2} + 1) + \sqrt{[\gamma(C_2 - C_1) + (\frac{R}{K_1} + 1)(\frac{R}{K_2} + 1)]^2 + 4\gamma C_1(\frac{R}{K_1} + 1)(\frac{R}{K_2} + 1)}}, \quad (\text{S27a})$$

$$\Xi_2^{\text{inter}}(RC_1, C_2)_0 = \frac{2k_2(R/K_1 + 1)/K_2}{\gamma(C_1 - C_2) + (\frac{R}{K_1} + 1)(\frac{R}{K_2} + 1) + \sqrt{[\gamma(C_1 - C_2) + (\frac{R}{K_1} + 1)(\frac{R}{K_2} + 1)]^2 + 4\gamma C_2(\frac{R}{K_1} + 1)(\frac{R}{K_2} + 1)}}, \quad (\text{S27b})$$

$$F_1^{\text{inter}}(RC_1, C_2)_0 = \frac{2k_1(R/K_2 + 1)R/K_1}{\gamma(C_2 - C_1) + (\frac{R}{K_1} + 1)(\frac{R}{K_2} + 1) + \sqrt{[\gamma(C_2 - C_1) + (\frac{R}{K_1} + 1)(\frac{R}{K_2} + 1)]^2 + 4\gamma C_1(\frac{R}{K_1} + 1)(\frac{R}{K_2} + 1)}}, \quad (\text{S27c})$$

$$F_2^{\text{inter}}(RC_1, C_2)_0 = \frac{2k_2(R/K_1 + 1)R/K_2}{\gamma(C_1 - C_2) + (\frac{R}{K_1} + 1)(\frac{R}{K_2} + 1) + \sqrt{[\gamma(C_1 - C_2) + (\frac{R}{K_1} + 1)(\frac{R}{K_2} + 1)]^2 + 4\gamma C_2(\frac{R}{K_1} + 1)(\frac{R}{K_2} + 1)}}. \quad (\text{S27d})$$

Since $\frac{4\gamma^2 C_1 C_2}{[\gamma C_1 + \gamma C_2 + (\frac{R}{K_1} + 1)(\frac{R}{K_2} + 1)]^2} < 1$, by applying first order approximation to the denominator of Eq. S26,

we obtain:

$$x_1 \approx \frac{C_1 R}{(R + K_1) + \frac{\gamma K_1 K_2 C_2}{(R+K_2)} - \frac{\gamma^2 K_1 K_2 C_1 C_2}{[\gamma(C_1+C_2)+(\frac{R}{K_1}+1)(\frac{R}{K_2}+1)](R+K_2)}}, \quad (S28a)$$

$$x_2 \approx \frac{C_2 R}{(R + K_2) + \frac{\gamma K_1 K_2 C_1}{(R+K_1)} - \frac{\gamma^2 K_1 K_2 C_1 C_2}{[\gamma(C_1+C_2)+(\frac{R}{K_1}+1)(\frac{R}{K_2}+1)](R+K_1)}}, \quad (S28b)$$

and the searching efficiencies and functional responses are

$$\Xi_1^{\text{inter}}(R, C_1, C_2)_{(2)} = \frac{k_1}{(R + K_1) + \frac{\gamma K_1 K_2 C_2}{(R+K_2)} - \frac{\gamma^2 K_1 K_2 C_1 C_2}{[\gamma(C_1+C_2)+(\frac{R}{K_1}+1)(\frac{R}{K_2}+1)](R+K_2)}}, \quad (S29a)$$

$$\Xi_2^{\text{inter}}(R, C_1, C_2)_{(2)} = \frac{k_2}{(R + K_2) + \frac{\gamma K_1 K_2 C_1}{(R+K_1)} - \frac{\gamma^2 K_1 K_2 C_1 C_2}{[\gamma(C_1+C_2)+(\frac{R}{K_1}+1)(\frac{R}{K_2}+1)](R+K_1)}}, \quad (S29b)$$

$$\mathcal{F}_1^{\text{inter}}(R, C_1, C_2)_{(2)} = \frac{k_1 R}{(R + K_1) + \frac{\gamma K_1 K_2 C_2}{(R+K_2)} - \frac{\gamma^2 K_1 K_2 C_1 C_2}{[\gamma(C_1+C_2)+(\frac{R}{K_1}+1)(\frac{R}{K_2}+1)](R+K_2)}}, \quad (S29c)$$

$$\mathcal{F}_2^{\text{inter}}(R, C_1, C_2)_{(2)} = \frac{k_2 R}{(R + K_2) + \frac{\gamma K_1 K_2 C_1}{(R+K_1)} - \frac{\gamma^2 K_1 K_2 C_1 C_2}{[\gamma(C_1+C_2)+(\frac{R}{K_1}+1)(\frac{R}{K_2}+1)](R+K_1)}}. \quad (S29d)$$

Likewise, the B-D model only fits to cases with $d = 0$. By calculating the average values in a stochastic framework, we obtain $\langle t_h^i \rangle = \frac{1}{k_i}$, $\langle t_w^i \rangle = \frac{1}{d'_{12}}$ ($i = 1, 2$). Then, we obtain the searching efficiencies in the B-D model:

$$\Xi_1^{\text{B-D (inter)}}(R, C_1, C_2) = \frac{a_1}{1 + \frac{a_1}{k_1} R + \frac{a'_{12}}{d'_{12}} C_2} = \frac{a_1}{1 + R/K_1 |_{d=0} + \gamma C_2}, \quad (S30a)$$

$$\Xi_2^{\text{B-D (inter)}}(R, C_1, C_2) = \frac{a_2}{1 + \frac{a_2}{k_2} R + \frac{a'_{12}}{d'_{12}} C_1} = \frac{a_2}{1 + R/K_2 |_{d=0} + \gamma C_1}. \quad (S30b)$$

Consequently, the functional responses in the B-D model are:

$$\mathcal{F}_1^{\text{B-D (inter)}}(R, C_1, C_2) = \frac{a_1 R}{1 + R/K_1 |_{d=0} + \gamma C_2}, \quad (S31a)$$

$$\mathcal{F}_2^{\text{B-D (inter)}}(R, C_1, C_2) = \frac{a_2 R}{1 + R/K_2 |_{d=0} + \gamma C_1}. \quad (S31b)$$

Evidently, the searching efficiencies in the B-D model are overall different from either the quasi-rigorous form $\Xi_i(R, C_1, C_2)_1$, or the simplified form $\Xi_i(R, C_1, C_2)_2$ (Appendix-fig. 2E-F). Still, the discrepancy can be small when $d \approx 0$ and $R \gg C$ (Appendix-fig. 2E-F). Intuitively, when $\gamma \ll \min(C_1^{-1}, C_2^{-1})$, we have

$$\Xi_1^{\text{inter}}(R, C_1, C_2)_{(2)} \approx \frac{a_1}{(1 + \frac{a_1}{k_1} R) + \frac{\gamma C_2}{R/K_2+1}}, \quad (S32a)$$

$$\Xi_2^{\text{inter}}(R, C_1, C_2)_{(2)} \approx \frac{a_2}{(1 + \frac{a_2}{k_2} R) + \frac{\gamma C_1}{R/K_1+1}}. \quad (S32b)$$

+ Thus, if $R/K_i = x_i/C_i^{(F)} < 1$ ($i = 1, 2$), then $\frac{1}{1+R/K_i} \in [0.5, 1]$. In this case, the difference between $\Xi_i^{\text{B-D (inter)}}(R, C_1, C_2)$ and $\Xi_i^{\text{inter}}(R, C_1, C_2)_{(2)}$ is small.

Appendix III Scenario involving chasing pair and intraspecific interference

A Two consumers species competing for one resource species

We consider the scenario involving chasing pair and intraspecific interference in the simple case of $S_C = 2$ and $S_R = 1$:

$$C_i^{(F)} + R^{(F)} \xrightleftharpoons[d_i]{a_i} C_i^{(P)} \vee R^{(P)} \xrightarrow{k_i} C_i^{(F)}(+),$$

$$C_i^{(F)} + C_i^{(F)} \xrightleftharpoons[d'_i]{a'_i} C_i^{(P)} \vee C_i^{(P)}, \quad i = 1, 2.$$

Here, the variables and parameters are just extended from the case of $S_C = 1$ and $S_R = 1$ (see Appendix II.). The total number of consumers and resources are $C_i \equiv C_i^{(F)} + x_i + 2y_i$ and $R \equiv R^{(F)} + \sum_{i=1}^2 x_i$. Hence, the population dynamics of the consumers and resources can be described as follows:

$$\begin{cases} \dot{x}_i = a_i C_i^{(F)} R^{(F)} - (k_i + d_i)x_i, \quad i = 1, 2; \\ \dot{y}_i = a'_i [C_i^{(F)}]^2 - d'_i y_i, \\ \dot{C}_i = w_i k_i x_i - D_i C_i, \\ \dot{R} = g(R, x_1, x_2, C_1, C_2). \end{cases} \quad (S33)$$

The functional form of $g(R, x_1, x_2, C_1, C_2)$ is unspecified. For simplicity, we limit our analysis to abiotic resources, while all results generically apply to biotic resources. Besides, we define $K_i \equiv (d_i + k_i)/a_i$, $\alpha_i \equiv D_i/(w_i k_i)$, and $\beta_i \equiv a'_i/d'_i$ ($i = 1, 2$). At steady state, from $\dot{x}_i = 0$, $\dot{y}_i = 0$, we have

$$\begin{cases} x_i = C_i^{(F)} R^{(F)} / K_i, \quad i = 1, 2; \\ y_i = \beta_i [C_i^{(F)}]^2. \end{cases} \quad (S34)$$

Note that $C_i \equiv C_i^{(F)} + x_i + 2y_i$, and $R \equiv R^{(F)} + \sum_{i=1}^2 x_i$. Then,

$$R^{(F)} = R / (1 + C_1^{(F)} / K_1 + C_2^{(F)} / K_2), \quad (S35a)$$

$$C_i = C_i^{(F)} + R^{(F)} C_i^{(F)} / K_i + 2\beta_i [C_i^{(F)}]^2, \quad i = 1, 2. \quad (S35b)$$

By substituting Eq. S35a into Eq. S35b, we have

$$C_2^{(F)} = \frac{K_2}{K_1} \left[\frac{R C_1^{(F)}}{C_1 - C_1^{(F)} - 2\beta_1 [C_1^{(F)}]^2} - K_1 - C_1^{(F)} \right], \quad (S36a)$$

$$(C_2 - C_2^{(F)} - 2\beta_2 [C_2^{(F)}]^2)(1 + C_1^{(F)} / K_1 + C_2^{(F)} / K_2) = R C_2^{(F)} / K_2. \quad (S36b)$$

Then, we can present $C_i^{(F)}$ with C_1 , C_2 and R ($i = 1, 2$). By further combining with Eqs. S34, S35a and S36a, we express $R^{(F)}$, x_i , and y_i using C_1 , C_2 and R . In particular, for x_i , we have:

$$x_i = u_i(R, C_1, C_2), \quad i = 1, 2. \quad (S37)$$

If all species coexist, then the steady-state equations of $\dot{C}_i = 0$ ($i = 1, 2$) and $\dot{R} = 0$ are:

$$\begin{cases} \Omega_1(R, C_1, C_2) - D_1 = 0, \\ \Omega_2(R, C_1, C_2) - D_2 = 0, \\ G(R, C_1, C_2) = 0, \end{cases} \quad (S38)$$

where $G(R, C_1, C_2) \equiv g(R, u_1(R, C_1, C_2), u_2(R, C_1, C_2), C_1, C_2)$, and $\Omega_i(R, C_1, C_2) \equiv \frac{w_i k_i}{C_i} u_i(R, C_1, C_2)$. In practice, Eq. S38 corresponds to three unparallel surfaces, which share a common point (Fig. 1H and Appendix-fig. 3D). Importantly, the fixed point can be stable, and hence two consumer species may coexist at constant population densities.

1 Stability analysis of the fixed-point solution

We use linear stability analysis to study the local stability of the fixed point. Specifically, for an arbitrary fixed point $E(x_1, x_2, y_1, y_2, C_1, C_2, R)$, only when all the eigenvalues (defined as $\lambda_i, i = 1, \dots, 7$) of the Jacobian matrix at point E own negative real parts would the point be locally stable.

To investigate whether there exists a non-zero measure parameter region for species coexistence, we set D_i ($i = 1, 2$) to be the only parameter that varies with species C_1 and C_2 , and then $\Delta \equiv (D_1 - D_2)/D_2$ reflects the competitive difference between the two consumer species. As shown in Appendix-fig. 4B, the region below the blue surface and above the red surface corresponds to stable coexistence. Thus, there exists a non-zero measure parameter region to promote species coexistence, which breaks CEP.

2 Analytical solutions of the species abundances at steady state

At steady state, since $\dot{x}_i = \dot{y}_i = \dot{C}_i = 0$ ($i = 1, 2$), then,

$$\begin{cases} x_i = \alpha_i C_i, \\ C_i^{(F)} = K_i \alpha_i C_i / R^{(F)}, \\ y_i = \beta_i (K_i \alpha_i C_i)^2 [R^{(F)}]^{-2}. \end{cases} \quad (S39)$$

Meanwhile, $C_i = C_i^{(F)} + x_i + 2y_i$, and $C_i, R > 0$ ($i = 1, 2$). Then, we have

$$C_i = \frac{(1 - \alpha_i)[R^{(F)}]^2 - K_i \alpha_i R^{(F)}}{2\beta_i (K_i \alpha_i)^2}. \quad (S40)$$

If the resource species owns a much larger population abundance than the consumers (i.e., $R \gg C_1 + C_2$), then $R \gg x_1 + x_2$, and $R^{(F)} \approx R$. Thus,

$$C_i = \frac{(1 - \alpha_i)R^2 - K_i \alpha_i R}{2\beta_i (K_i \alpha_i)^2}. \quad (S41)$$

By further assuming that the population dynamics of the resources follow identical construction rule as the MacArthur's consumer-resource model (*MacArthur, 1970*), we have

$$g(R, x_1, x_2, C_1, C_2) = R_a(1 - R/K_0) - (k_1 x_1 + k_2 x_2). \quad (S42)$$

Since $\dot{R} = 0$, then

$$R = \frac{-\kappa_1 + \sqrt{\kappa_1^2 + 4\kappa_2 R_a}}{2\kappa_2}, \quad (S43)$$

where $\kappa_1 = \frac{R_a}{K_0} - \frac{k_1}{2\beta_1 K_1} - \frac{k_2}{2\beta_2 K_2}$ and $\kappa_2 = \frac{k_1(1-\alpha_1)}{2\beta_1 \alpha_1 (K_1)^2} + \frac{k_2(1-\alpha_2)}{2\beta_2 \alpha_2 (K_2)^2}$.

Eqs. S41, S43 are the analytical solutions of species abundances at steady state when $R \gg C_1 + C_2$. As shown in Fig. 1E, the analytical solutions agree well with the numerical results (the exact solutions). To conduct a systematic comparison for different model parameters, we assign D_i ($i = 1, 2$) to be the only parameter varying with species C_1 and C_2 ($D_1 > D_2$), and define $\Delta \equiv (D_1 - D_2)/D_2$ as the competitive difference between the two consumer species. The comparison between analytical solutions and numerical results is shown in Appendix-fig. 3E. Clearly, they are close to each other, exhibiting very good consistency.

Furthermore, we test if the parameter region for species coexistence is predictable using the analytical solutions. Since D_i ($i = 1, 2$) is the only parameter that varies with the two-consumer species, the supremum of the tolerated competitive difference for species coexistence (defined as $\bar{\Delta}$) corresponds to the steady-state solutions that satisfy $R, C_2 > 0$ and $C_1 = 0^+$, where 0^+ stands for the infinitesimal positive number. To calculate the analytical solutions at the upper surface of the coexistence region, where $\Delta = \bar{\Delta}$ and $C_1 = 0^+$, we further combine Eq. S41 and then obtain (note that $R > 0$)

$$R = \frac{K_1 \alpha_1}{1 - \alpha_1}. \quad (S44)$$

Meanwhile,

$$\alpha_1 = \alpha_2(\Delta + 1) = \alpha_2(\bar{\Delta} + 1). \quad (S45)$$

Combining Eqs. S43-S45, we have

$$\bar{\Delta} = \frac{1}{\alpha_2(K_1\varpi + 1)} - 1, \quad (S46)$$

where $\varpi = \frac{1}{2}(\frac{1}{K_0} - \frac{k_2}{2R_a\beta_2K_2}) + \frac{1}{2}\sqrt{(\frac{1}{K_0} - \frac{k_2}{2R_a\beta_2K_2})^2 + 2\frac{k_2(1-\alpha_2)}{R_a\beta_2\alpha_2(K_2)^2}}$. When $R \gg C_1 + C_2$, the comparison of $\bar{\Delta}$ obtained from analytical solutions with that from numerical results (the exact solutions) are shown in Appendix-fig. 3F, which overall exhibits good consistency.

B S_C consumers species competing for S_R resources species

Here we consider the scenario involving chasing pair and intraspecific interference for the generic case with S_C types of consumers and S_R types of resources. Then, the population dynamics of the system can be described as follows:

$$\begin{cases} \dot{x}_{il} = a_{il}C_i^{(F)}R_l^{(F)} - (k_{il} + d_{il})x_{il}, \\ \dot{y}_i = a'_{ii}[C_i^{(F)}]^2 - d'_{ii}y_i, \\ \dot{C}_i = \sum_{l=1}^{S_R} w_{il}k_{il}x_{il} - D_iC_i, \\ \dot{R}_l = g_l(\{R_l\}, \{x_i\}, \{C_i\}), i = 1, \dots, S_C, l = 1, \dots, S_R. \end{cases} \quad (S47)$$

Note that Eq. S47 is identical with Eqs. 1-2, and we use the same variables and parameters as that in the main text. Then, the populations of the consumers and resources are $C_i = C_i^{(F)} + \sum_{l=1}^{S_R} x_{il} + 2y_i$ and $R_l = R_l^{(F)} + \sum_{i=1}^{S_C} x_{il}$. For convenience, we define $K_{il} \equiv (d_{il} + k_{il})/a_{il}$, $\alpha_{il} \equiv D_{il}/(k_{il}w_{il})$ and $\beta_i \equiv a'_{ii}/d'_{ii}$ ($i = 1, \dots, S_C, l = 1, \dots, S_R$).

1 Analytical solutions of species abundances at steady state

At steady state, from $\dot{x}_{il} = 0$, $\dot{y}_i = 0$, and $\dot{C}_i = 0$, we have,

$$\begin{cases} x_{il} = C_i^{(F)}R_l^{(F)}/K_{il}, \\ y_i = \beta_i[C_i^{(F)}]^2, \\ C_i = \sum_{l=1}^{S_R} x_{il}/\alpha_{il} = \sum_{l=1}^{S_R} C_i^{(F)}R_l^{(F)}/(K_{il}\alpha_{il}). \end{cases} \quad (S48)$$

Meanwhile $C_i = C_i^{(F)} + \sum_{l=1}^{S_R} x_{il} + 2y_i$, and note that $C_i > 0$, thus

$$C_i^{(F)} = \frac{1}{2\beta_i}[-1 + \sum_{l=1}^{S_R}(\frac{1}{\alpha_{il}} - 1)\frac{R_l^{(F)}}{K_{il}}]. \quad (S49)$$

Combined with Eq. S49, and then

$$C_i = \sum_{l=1}^{S_R} \frac{R_l^{(F)}}{2\beta_i\alpha_{il}K_{il}}[-1 + \sum_{l'=1}^{S_R}(\frac{1}{\alpha_{il'}} - 1)\frac{R_{l'}^{(F)}}{K_{il'}}]. \quad (S50)$$

We further assume that the specific function of $g_l(\{R_l\}, \{x_i\}, \{C_i\})$ satisfies Eq. 4, i.e.,

$$g_l(\{R_l\}, \{x_i\}, \{C_i\}) = R_a^{(l)}(1 - R_l/K_0^{(l)}) - \sum_{i=1}^{S_C} k_{il}x_{il}. \quad (S51)$$

By combining Eqs. S48, S49 and S51, we have

$$R_a^{(l)}(1 - \frac{R_l}{K_0^{(l)}}) = \sum_{i=1}^{S_C} \frac{k_{il}}{2\beta_iK_{il}}[-1 + \sum_{l'=1}^{S_R}(\frac{1}{\alpha_{il'}} - 1)\frac{R_{l'}^{(F)}}{K_{il'}}]R_l^{(F)}. \quad (S52)$$

If the population abundance of each resource species is much more than the total population of all consumers (i.e., $R_l \gg \sum_{i=1}^{S_C} C_i (l = 1, \dots, S_R)$), then $R_l \gg \sum_{i=1}^{S_C} x_{il}$ and $R_l^{(F)} \approx R_l$. Thus,

$$\left(\frac{R_a^{(l)}}{K_0^{(l)}} - \sum_{i=1}^{S_C} \frac{k_{il}}{2\beta_i K_{il}} + \sum_{l'=1}^{S_R} \sum_{i=1}^{S_C} \frac{k_{il}}{2\beta_i K_{il}} \left(\frac{1}{\alpha_{il'}} - 1 \right) \frac{R_{l'}}{K_{il'}} \right) R_l = R_a^{(l)}, \quad (S53)$$

with $l = 1, \dots, S_R$. Eq. S53 is a set of second-order algebraic differential equations, which is clearly solvable.

In fact, when $S_R = 1, S_C \geq 1$, and $R_l \gg \sum_{i=1}^{S_C} C_i (l = 1)$, we can explicitly present the analytical solution of the steady-state species abundances. To simplify the notations, we omit the “ l ” in the sub-/super-scripts since $S_R = 1$. Then, we have

$$\begin{cases} R = \frac{-\gamma_1 + \sqrt{\gamma_1^2 + 4\gamma_2 R_a}}{2\gamma_2}, \\ C_i = \frac{1}{2\beta_i \alpha_i K_i} \left[\left(\frac{1}{\alpha_i} - 1 \right) \frac{R}{K_i} - 1 \right] R, \quad i = 1, \dots, S_C. \end{cases} \quad (S54)$$

Here $\gamma_1 \equiv \frac{R_a}{K_0} - \sum_{i=1}^{S_C} \frac{k_i}{2\beta_i K_i}$ and $\gamma_2 \equiv \sum_{i=1}^{S_C} \frac{k_i(1-\alpha_i)}{2\beta_i \alpha_i (K_i)^2}$.

C Intuitive understanding: an underlying negative feedback loop

Intuitively, how can intraspecific predator interference promote biodiversity? Here we solve this question by considering the case that S_C types of consumers compete for one resource species. The population dynamics of the system are described in Eqs. S47 and S51 with $S_R = 1$. To simplify the notations, we omit the “ l ” in the subscript since $S_R = 1$. The consumption process and interference process are supposed to be in fast equilibrium (i.e., $\dot{x}_i = 0, \dot{y}_i = 0$). Then, we have a set of equations to solve for x_i and y_i given the population size of each species:

$$\begin{cases} x_i = C_i^{(F)} R^{(F)} / K_i, \\ y_i = \beta_i [C_i^{(F)}]^2, \\ C_i = C_i^{(F)} + x_i + 2y_i, \\ R = R^{(F)} + \sum_{i=1}^{S_C} x_i. \end{cases} \quad (S55)$$

In the first three sub-equations of Eq. S55, by getting rids of $C_i^{(F)}$, we have,

$$\begin{cases} 2\beta_i \left[\frac{x_i}{R^{(F)}} \right]^2 + x_i + \frac{K_i x_i}{R^{(F)}} - C_i = 0, \\ y_i = \frac{1}{2} \left[C_i - x_i - \frac{x_i}{R^{(F)}} \right]. \end{cases} \quad (S56)$$

Then, by regarding $R^{(F)}$ as a temporary parameter, we solve for x_i and y_i :

$$\begin{cases} x_i = \frac{2R^{(F)} C_i}{\sqrt{(R^{(F)} + K_i)^2 + 8\beta_i K_i^2 C_i + R^{(F)} + K_i}}, \\ y_i = \frac{1}{2} \left[C_i - \left(1 + \frac{K_i}{R^{(F)}} \right) x_i \right]. \end{cases} \quad (S57)$$

If the total population size of the resources is much larger than that of consumers (i.e., $R \gg \sum_{i=1}^{S_C} C_i$),

then $R \gg \sum_{i=1}^{S_C} x_i$ and $R^{(F)} \approx R$, and thus we get the analytical expressions of x_i and y_i

$$\begin{cases} x_i \approx \frac{2RC_i}{\sqrt{(R+K_i)^2 + 8\beta_i K_i^2 C_i + R + K_i}}, \\ y_i \approx \frac{C_i}{2} \left[1 - \frac{2(R+K_i)}{\sqrt{(R+K_i)^2 + 8\beta_i K_i^2 C_i + R + K_i}} \right]. \end{cases} \quad (S58)$$

Note that the fraction of C_i individuals engaged in chasing pairs is x_i/C_i , while that for individuals trapped in intraspecific interference pairs is y_i/C_i . With Eq. S58, it is straightforward to obtain these fractions:

$$\begin{cases} x_i/C_i \approx \frac{2R}{\sqrt{(R+K_i)^2 + 8\beta_i K_i^2 C_i + R + K_i}}, \\ y_i/C_i \approx \frac{1}{2} \left(1 - \frac{2(R+K_i)}{\sqrt{(R+K_i)^2 + 8\beta_i K_i^2 C_i + R + K_i}} \right). \end{cases} \quad (\text{S59})$$

where both x_i/C_i and y_i/C_i are bivariate functions of R and C_i . From Eq. S59, it is clear that for a given population size of the resource species, y_i/C_i is a monotonously increasing function of C_i , while x_i/C_i is a monotonously decreasing function of C_i . In Appendix-fig. 15A-B, we see that the analytical results are highly consistent with the exact numerical solutions. By definition, the functional response of C_i species is $\mathcal{F} \equiv k_i x_i/C_i$, and thus,

$$\mathcal{F}(R, C_i) \approx \frac{2R}{\sqrt{(R+K_i)^2 + 8\beta_i K_i^2 C_i + R + K_i}}, \quad (\text{S60})$$

Evidently, the function response of C_i species is negatively correlated with the population size of itself, which effectively constitutes a self-inhibiting negative feedback loop (Appendix-fig. 15C).

Then, we have a simple intuitive understanding of species coexistence through the mechanism of intraspecific interference. In an ecological community, consumer species that of higher/lower competitiveness tend to increase/decrease their population size in the competition process. Without intraspecific interference, the increasing/decreasing trend would continue until the system obeys CEP. In the scenario involving intraspecific interference, however, for species of higher competitiveness (e.g., C_i), with the increase of C_i 's population size, a larger portion of C_i individuals are then engaged in intraspecific interference pair which are temporarily absent from hunting (Appendix-fig. 15A-B). Consequently, the functional response of C_i drops, which prevents further increase of C_i 's population size, results in an overall balance among the consumer species, and thus promotes species coexistence.

Appendix IV Scenario involving chasing pair and interspecific interference

Here we consider the scenario involving chasing pair and interspecific interference in the case of $S_C = 2$ and $S_R = 1$, with all settings follow that depicted in Appendix II. . Then, $C_i \equiv C_i^{(F)} + x_i + z$, $R \equiv R^{(F)} + x_1 + x_2$, and the population dynamics follows (identical with Eq. S25):

$$\begin{cases} \dot{x}_i = a_i C_i^{(F)} R^{(F)} - (k_i + d_i) x_i, i = 1, 2; \\ \dot{z} = a'_{12} C_1^{(F)} C_2^{(F)} - d'_{12} z, \\ \dot{C}_i = w_i k_i x_i - D_i C_i, \\ \dot{R} = g(R, x_1, x_2, C_1, C_2). \end{cases} \quad (\text{S61})$$

Here the functional form of $g(R, x_1, x_2, C_1, C_2)$ is unspecified. For convenience, we define $K_i \equiv (d_i + k_i)/a_i$, $\alpha_i \equiv D_i/(w_i k_i)$ ($i = 1, 2$), and $\gamma \equiv a'_{12}/d'_{12}$. At steady state, from $\dot{x}_i = 0$ ($i = 1, 2$) and $\dot{z} = 0$, we have

$$\begin{cases} x_i = C_i^{(F)} R^{(F)} / K_i, i = 1, 2; \\ z = \gamma C_1^{(F)} C_2^{(F)}. \end{cases} \quad (\text{S62})$$

Note that $C_i \equiv C_i^{(F)} + x_i + z$ and $R \equiv R^{(F)} + x_1 + x_2$, then,

$$\begin{cases} C_1 = C_1^{(F)} + R^{(F)} C_1^{(F)} / K_1 + \gamma C_1^{(F)} C_2^{(F)}, \\ C_2 = C_2^{(F)} + R^{(F)} C_2^{(F)} / K_2 + \gamma C_1^{(F)} C_2^{(F)}, \\ R = R^{(F)} (1 + C_1^{(F)} / K_1 + C_2^{(F)} / K_2). \end{cases} \quad (\text{S63})$$

Then, we can express $C_1^{(F)}$, $C_2^{(F)}$ and $R^{(F)}$ with C_1 , C_2 and R . Combined with Eq. S62, x_i and z can also be expressed using C_1 , C_2 and R . In particular, for x_i , we have

$$x_i = u'_i(R, C_1, C_2), i = 1, 2. \quad (S64)$$

If all species coexist, by defining $\Omega'_i(R, C_1, C_2) \equiv \frac{u_i k_i}{C_i} u'_i(R, C_1, C_2)$, then, the steady-state equations of $\dot{C}_i = 0$ ($i = 1, 2$) and $\dot{R} = 0$ are:

$$\begin{cases} \Omega'_1(R, C_1, C_2) - D_1 = 0, \\ \Omega'_2(R, C_1, C_2) - D_2 = 0, \\ G'(R, C_1, C_2) = 0, \end{cases} \quad (S65)$$

where $G'(R, C_1, C_2) \equiv g(R, u'_1(R, C_1, C_2), u'_2(R, C_1, C_2), C_1, C_2)$.

Here, Eq. S65 corresponds to three unparallel surfaces and share a common point (Fig. 1G and Appendix-fig 3A). However, all the fixed points are unstable (Appendix-fig. 3C), and hence the consumer species cannot stably coexist at steady state (Fig. 1D).

A Analytical results of the fixed-point solution

We proceed to investigate the unstable fixed point where $R, C_1, C_2 > 0$. From $\dot{x}_i = 0$ ($i = 1, 2$), $\dot{z} = 0$, $\dot{C}_i = 0$, and note that $C_i \equiv C_i^{(F)} + x_i + z$, we have

$$\begin{cases} C_i = K_i \alpha_i C_i (R^{(F)})^{-1} + \alpha_i C_i + z, i = 1, 2; \\ z = \gamma K_1 \alpha_1 K_2 \alpha_2 (R^{(F)})^{-2} C_1 C_2. \end{cases} \quad (S66)$$

Since $C_i > 0$, then

$$\begin{cases} C_1 = \frac{(1-\alpha_2)[R^{(F)}]^2 - K_2 \alpha_2 R^{(F)}}{\gamma K_1 \alpha_1 K_2 \alpha_2}, \\ C_2 = \frac{(1-\alpha_1)[R^{(F)}]^2 - K_1 \alpha_1 R^{(F)}}{\gamma K_1 \alpha_1 K_2 \alpha_2}. \end{cases} \quad (S67)$$

If $R \gg C_1 + C_2$, then $R \gg x_1 + x_2$ and $R^{(F)} \approx R$, we have

$$\begin{cases} C_1 = \frac{(1-\alpha_2)R^2 - K_2 \alpha_2 R}{\gamma K_1 \alpha_1 K_2 \alpha_2}, \\ C_2 = \frac{(1-\alpha_1)R^2 - K_1 \alpha_1 R}{\gamma K_1 \alpha_1 K_2 \alpha_2}. \end{cases} \quad (S68)$$

Still, we assume that the population dynamics of the resource species follows Eq. S42. At the fixed point, $\dot{R} = 0$. We have

$$R_a \left(1 - \frac{R}{K_0}\right) = k_1 \alpha_1 C_1 + k_2 \alpha_2 C_2. \quad (S69)$$

Combined with Eq. S68, we can solve for R

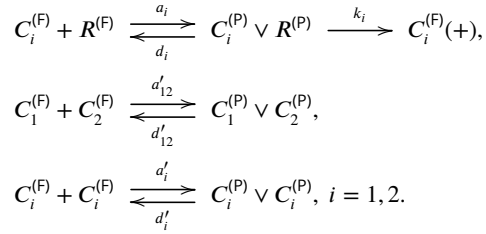
$$R = \frac{-\varrho_1 + \sqrt{\varrho_1^2 + 4\varrho_2 R_a}}{2\varrho_2}. \quad (S70)$$

where $\varrho_1 = \frac{R_a}{K_0} - \frac{k_1}{\gamma K_1} - \frac{k_2}{\gamma K_2}$ and $\varrho_2 = \frac{k_1(1-\alpha_2)}{\gamma K_1 K_2 \alpha_2} + \frac{k_2(1-\alpha_1)}{\gamma K_1 K_2 \alpha_1}$.

Eqs. S68, S70 are the analytical solutions of the fixed point when $R \gg C_1 + C_2$. As shown in Appendix-fig. 3B, the analytical predictions agree well with the numerical results (the exact solutions).

Appendix V Scenario involving chasing pair and both intra- and inter-specific interference

Here we consider the scenario involving chasing pair and both intra- and inter-specific interference in the simple case of $S_C = 2$ and $S_R = 1$:



We adopt the same notations as that depicted in Appendix III. and . Then, $C_i \equiv C_i^{(F)} + x_i + 2y_i + z$ and $R \equiv R^{(F)} + x_1 + x_2$, and the population dynamics of the system can be described as follows:

$$\begin{cases} \dot{x}_i = a_i C_i^{(F)} R^{(F)} - (k_i + d_i) x_i, \\ \dot{z} = a'_{12} C_1^{(F)} C_2^{(F)} - d'_{12} z, \\ \dot{y}_i = a'_i [C_i^{(F)}]^2 - d'_i y_i, \\ \dot{C}_i = w_i k_i x_i - D_i C_i, \\ \dot{R} = g(R, x_1, x_2, C_1, C_2), \quad i = 1, 2. \end{cases} \quad (S71)$$

Here, the functional form of $g(R, x_1, x_2, C_1, C_2)$ follows Eq. S42. For convenience, we define $K_i \equiv (d_i + k_i)/a_i$, $\alpha_i \equiv D_i/(w_i k_i)$, $\beta_i \equiv a'_i/d'_i$, and $\gamma \equiv a'_{12}/d'_{12}$, ($i = 1, 2$). At steady state, from $\dot{x}_i = 0$, $\dot{y}_i = 0$, $\dot{z} = 0$, and $\dot{C}_i = 0$, ($i = 1, 2$), we have

$$\begin{cases} x_i = \alpha_i C_i, \\ C_i^{(F)} = K_i \alpha_i C_i (R^{(F)})^{-1}, \\ y_i = \beta_i (K_i \alpha_i C_i)^2 [R^{(F)}]^{-2}, \\ z = \gamma K_1 \alpha_1 K_2 \alpha_2 [R^{(F)}]^{-2} C_1 C_2. \end{cases} \quad (S72)$$

Combined with $C_i \equiv C_i^{(F)} + x_i + 2y_i + z$, and since $C_i > 0$ ($i = 1, 2$), then,

$$\begin{cases} (1 - \alpha_1)(R^{(F)})^2 - K_1 \alpha_1 R^{(F)} = 2\beta_1 (K_1 \alpha_1)^2 C_1 + \gamma K_1 \alpha_1 K_2 \alpha_2 C_2, \\ (1 - \alpha_2)(R^{(F)})^2 - K_2 \alpha_2 R^{(F)} = 2\beta_2 (K_2 \alpha_2)^2 C_2 + \gamma K_1 \alpha_1 K_2 \alpha_2 C_1. \end{cases} \quad (S73)$$

A Analytical solutions of species abundances at steady state

If $R \gg C_1 + C_2$, then $R \gg x_1 + x_2$ and thus $R^{(F)} \approx R$. Combined with Eq. S73, we obtain

$$\begin{cases} C_1 = R \frac{(2\beta_2 K_2 \alpha_2 (1 - \alpha_1) - \gamma K_1 \alpha_1 (1 - \alpha_2)) R + (\gamma - 2\beta_2) K_1 \alpha_1 K_2 \alpha_2}{K_1^2 \alpha_1^2 K_2 \alpha_2 (4\beta_1 \beta_2 - \gamma^2)}, \\ C_2 = R \frac{(2\beta_1 K_1 \alpha_1 (1 - \alpha_2) - \gamma K_2 \alpha_2 (1 - \alpha_1)) R + (\gamma - 2\beta_1) K_1 \alpha_1 K_2 \alpha_2}{K_1 \alpha_1 K_2^2 \alpha_2^2 (4\beta_1 \beta_2 - \gamma^2)}. \end{cases} \quad (S74)$$

Using $\dot{R} = 0$ and $R > 0$, we have

$$R = \frac{-\kappa'_2 + \sqrt{(\kappa'_2)^2 + 4\kappa'_1 R_a}}{2\kappa'_1}, \quad (S75)$$

where $\kappa'_1 = \frac{k_2 \gamma (\alpha_1 - 1)}{K_1 K_2 \alpha_1 (4\beta_1 \beta_2 - \gamma^2)} + \frac{k_1 \gamma (\alpha_2 - 1)}{K_1 K_2 \alpha_2 (4\beta_1 \beta_2 - \gamma^2)} - \frac{k_1 2\beta_2 (\alpha_1 - 1)}{K_1^2 \alpha_1 (4\beta_1 \beta_2 - \gamma^2)} - \frac{k_2 2\beta_1 (\alpha_2 - 1)}{K_2^2 \alpha_2 (4\beta_1 \beta_2 - \gamma^2)}$, and $\kappa'_2 = \frac{k_1 (\gamma - 2\beta_2)}{K_1 (4\beta_1 \beta_2 - \gamma^2)} + \frac{k_2 (\gamma - 2\beta_1)}{K_2 (4\beta_1 \beta_2 - \gamma^2)} + \frac{R_a}{K_0}$. Eqs. S74-S75 are the analytical solutions of the species abundances at steady state when $R \gg C_1 + C_2$. As shown in Appendix-fig. 5E, the analytical calculations agree well with the numerical results (the exact solutions).

B Stability analysis of the coexisting state

In the scenario involving chasing pair and both intra- and inter-specific interference, the behavior of species coexistence is similar to that without interspecific interference. Evidently, the influence of interspecific interference would be negligible if d'_{12} is extremely large, and vice versa for intraspecific interference if both d'_1 and d'_2 are tremendous. In the deterministic framework, the two-consumer species may coexist at constant population densities (Appendix-fig. 5B), and the fixed points are globally attracting (Appendix-fig. 5C). Furthermore, there is a non-zero measure of parameter set where both consumer species can coexist at steady state with only one type of resources (Appendix-fig. 5A). In the stochastic framework, just as the scenario involving chasing pair and intraspecific interference, the coexistence state can be maintained along with stochasticity (Appendix-fig. 5D).

Appendix VI Dimensional analysis for the scenario involving chasing pair and both intra- and inter-specific interference

The population dynamics of the system involving chasing pair and both intra- and inter-specific interference are shown in Eqs. 1-4:

$$\begin{cases} \dot{x}_{il} = a_{il}C_i^{(F)}R_l^{(F)} - (d_{il} + k_{il})x_{il}, \\ \dot{y}_i = a'_i[C_i^{(F)}]^2 - d'_iy_i, \\ \dot{z}_{ij} = a'_{ij}C_i^{(F)}C_j^{(F)} - d'_{ij}z_{ij} \\ \dot{C}_i = \sum_{l=1}^{S_R} w_{il}k_{il}x_{il} - D_iC_i, \\ \dot{R}_l = R_a^{(l)}(1 - R_l/K_0^{(l)}) - \sum_{i=1}^{S_C} k_{il}x_{il}, \end{cases} \quad (S76)$$

with $l = 1, \dots, S_R$; $i, j = 1, \dots, S_C$, and $i \neq j$. Here $C_i = C_i^{(F)} + \sum_l x_{il} + 2y_i + \sum_{i \neq j} z_{ij}$ and $R_l = R_l^{(F)} + \sum_i x_{il}$ represent the population abundances of the consumers and resources in the system. In fact, there are already several dimensionless variables and parameter in Eq. S76, namely x_{il} , y_i , z_{ij} , $C_i^{(F)}$, $R_l^{(F)}$, C_i , R_l , w_{il} , $K_0^{(l)}$. To make all terms dimensionless, we define $\tilde{t} = t/\tau$, where $\tau = \tilde{D}_1/D_1$ and \tilde{D}_1 is a reducible dimensionless parameter which is freely to take any positive values. Besides, we define dimensionless parameters $\tilde{a}_{il} = a_{il}\tau$, $\tilde{d}_{il} = d_{il}\tau$, $\tilde{k}_{il} = k_{il}\tau$, $\tilde{a}'_i = a'_i\tau$, $\tilde{d}'_i = d'_i\tau$, $\tilde{a}'_{ij} = a'_{ij}\tau$, $\tilde{d}'_{ij} = d'_{ij}\tau$, $\tilde{D}_i = D_i\tau$ and $\tilde{R}_a^{(l)} = R_a^{(l)}\tau$. By substituting all the dimensionless terms into Eq. S76, we have

$$\begin{cases} \dot{x}_{il} = \tilde{a}_{il}C_i^{(F)}R_l^{(F)} - (\tilde{d}_{il} + \tilde{k}_{il})x_{il}, \\ \dot{y}_i = \tilde{a}'_i[C_i^{(F)}]^2 - \tilde{d}'_iy_i, \\ \dot{z}_{ij} = \tilde{a}'_{ij}C_i^{(F)}C_j^{(F)} - \tilde{d}'_{ij}z_{ij} \\ \dot{C}_i = \sum_{l=1}^{S_R} w_{il}\tilde{k}_{il}x_{il} - \tilde{D}_iC_i, \\ \dot{R}_l = \tilde{R}_a^{(l)}(1 - R_l/K_0^{(l)}) - \sum_{i=1}^{S_C} \tilde{k}_{il}x_{il}. \end{cases} \quad (S77)$$

For convenience, we omit the notation “~” and use dimensionless variables and parameters in the simulation studies unless otherwise specified.

Appendix VII Simulation details of the main text figures

In Fig. 1C, F: $a_i = 0.1$, $d_i = 0.5$, $w_i = 0.1$, $k_i = 0.1$ ($i = 1, 2$); $D_1 = 0.002$, $D_2 = 0.001$, $K_0 = 5$, $R_a = 0.05$. In Fig. 1D, G: $a_i = 0.02$, $a'_{ij} = 0.021$, $d_i = 0.5$, $d'_{ij} = 0.01$, $w_i = 0.08$, $k_i = 0.03$, $i, j = 1, 2$, $i \neq j$, $D_2 = 0.001$, $D_1 = 0.0011$, $K_0 = 20$, $R_a = 0.01$. In Fig. 1E, H: $a_i = 0.5$, $a'_i = 0.525$, $d_i = 0.5$, $d'_i = 0.5$, $w_i = 0.2$, $k_i = 0.4$ ($i = 1, 2$), $D_1 = 0.022$, $D_2 = 0.020$, $K_0 = 10$, $R_a = 0.1$. Fig. 1C, F were calculated or simulated from Eqs. 1, 4. Fig. 1D, G were calculated or simulated from Eqs. 1, 3, 4. Fig. 1E, H were calculated or simulated from Eqs. 1, 2, 4. The analytical solutions in Fig. 1E were calculated from Eqs. S41 and S43.

In Fig. 2A: $a_i = 0.02, a'_i = 0.025, d_i = 0.7, d'_i = 0.7, w_i = 0.4, k_i = 0.05$ ($i = 1, 2$); $D_1 = 0.0160, D_2 = 0.0171, K_0 = 2000, R_a = 5.5$. In Fig. 2B-C: $L = 100, r^{(C)} = 5, r^{(O)} = 5, v_{C_i} = 1, v_R = 0.1, a_i = 0.2010, a'_i = 0.2828, d'_i = 0.8, d_i = 0.7, w_i = 0.33, k_i = 0.2$ ($i = 1, 2$); $D_1 = 0.0605, D_2 = 0.0600, K_0 = 1000, R_a = 100$. In Fig. 2D: $a_i = 0.3, a'_i = 0.33, w_i = 0.018, k_i = 4.8, d'_i = 5, d_i = 5.5$ ($i = 1, 2$); $D_2 = 0.010, R_a = 35, K_0 = 10000, D_1 = 0.011$. In Fig. 2E: $w_i = 0.02, k_i = 4.5, d'_i = 4, d_i = 4.5$ ($i = 1, 2$); $D_2 = 0.010, R_a = 35, K_0 = 10000, a_i = 0.2, a'_i = 0.24$ ($i = 1, 2$); $D_1 = 0.0120$. In Fig. 2D-E: $\tau = 0.4\text{Day}$ (see). Fig. 2A-E were simulated from Eqs. 1, 2, 4. See Appendix-fig. 7C, E for the long-term time series of all species in Fig. 2D-E, respectively.

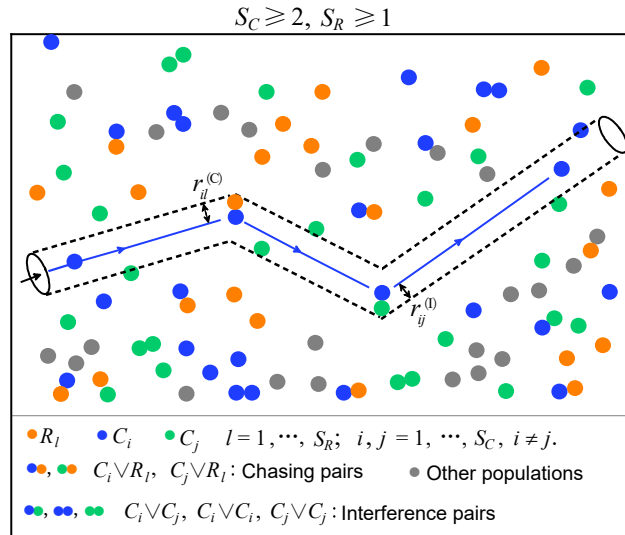
Model settings in Fig. 3A-B, D (plankton): $a_{i1} = 0.1, a'_i = 0.125, d_{i1} = 0.5, d'_i = 0.2, w_{i1} = 0.3, k_{i1} = 0.2, K_0^{(1)} = 8 \times 10^4, K_0^{(2)} = 5 \times 10^4, K_0^{(3)} = 3 \times 10^4, R_a^{(1)} = 280, R_a^{(2)} = 200, R_a^{(3)} = 150, D_i = 0.03 \times \mathcal{N}(1, 0.25)$ ($i = 1, \dots, S_C, l = 1, \dots, S_R$), $S_C = 140$ and $S_R = 3$. Model settings in Fig. 3C (bird): $a_i = 0.1, a'_i = 0.125, d_i = 0.5, d'_i = 0.5, w_i = 0.3, k_i = 0.2, D_i = 0.02 \times \mathcal{N}(1, 0.28)$ ($i = 1, \dots, S_C$); $R_a = 110, K_0 = 10^5, S_C = 250$ and $S_R = 1$. Model settings in Fig. 3C (fish): $a_i = 0.1, a'_i = 0.14, d_i = 0.5, d'_i = 0.5, w_i = 0.2, k_i = 0.1, D_i = 0.015 \times \mathcal{N}(1, 0.32)$ ($i = 1, \dots, 45$); $R_a = 550, K_0 = 10^6, S_C = 45$ and $S_R = 1$. Model settings in Fig. 3C (butterfly): $a_i = 0.1, a'_i = 0.125, d_i = 0.5, d'_i = 0.3, w_i = 0.3, k_i = 0.2, D_i = 0.034 \times \mathcal{N}(1, 0.35)$ ($i = 1, \dots, S_C$); $R_a = 300, K_0 = 10^5, S_C = 150$ and $S_R = 1$. Model settings in Fig. 3D (bat): $a_i = 0.1, a'_i = 0.125, d_i = 0.5, d'_i = 0.5, w_i = 0.2, k_i = 0.1, D_i = 0.013 \times \mathcal{N}(1, 0.34)$ ($i = 1, \dots, S_C$); $R_a = 250, K_0 = 10^6, S_C = 40$ and $S_R = 1$. Model settings in Fig. 3D (lizard): $a_i = 0.1, a'_i = 0.125, d_i = 0.5, d'_i = 0.5, w_i = 0.2, k_i = 0.1, D_i = 0.014 \times \mathcal{N}(1, 0.34)$ ($i = 1, \dots, S_C$); $R_a = 250, K_0 = 10^6, S_C = 55$ and $S_R = 1$. In Fig. 3A-D, the mortality rate D_i ($i = 1, \dots, S_C$) is the only parameter that varies with the consumer species, which was randomly sampled from a Gaussian distribution $\mathcal{N}(\mu, \sigma)$, where μ and σ are the mean and standard deviation of the distribution. The coefficient of variation of the mortality rates (i.e., σ/μ) was chosen to be around 0.3, or more precisely, the best-fit in the range of 0.15-0.43. This range was estimated from experimental results (Menon et al., 2003) using the two-sigma rule. These settings for the mortality rates also apply to those in Appendix-figs. 8-14. Fig. 3A-D were simulated from Eqs. 1, 2, 4. See Appendix-figs. 14C, 10K, C, D, H, I, J, Fig. 3A, Fig. 3B for the time series of Fig. 3C (ODEs $^{S_R=1}_{\text{bird}}$), 3C (ODEs $^{S_R=1}_{\text{butterfly}}$), 3C (ODEs $^{S_R=1}_{\text{fish}}$), 3D (ODEs $^{S_R=1}_{\text{bat}}$), 3D (SSA $^{S_R=1}_{\text{bat}}$), 3D (ODEs $^{S_R=1}_{\text{lizard}}$), 3D (SSA $^{S_R=1}_{\text{lizard}}$), 3D (ODEs $^{S_R=3}_{\text{plankton}}$) and 3D (SSA $^{S_R=3}_{\text{plankton}}$), respectively. The Shannon entropies of the experimental data and simulation results for each ecological community are: $H_{\text{Exp(ODEs)}}^{\text{bird(1982)}} = 5.67(6.79)$, $H_{\text{Exp(ODEs)}}^{\text{bird(2018)}} = 6.63(6.79)$, $H_{\text{Exp(ODEs)}}^{\text{butterfly}} = 4.78(4.12)$, $H_{\text{Exp(ODEs)}}^{\text{fish}} = 3.78(3.40)$; $H_{\text{Exp(ODEs,SSA)}}^{\text{bat}} = 3.00(2.95, 2.84)$, $H_{\text{Exp(ODEs,SSA)}}^{\text{lizard}} = 4.05(3.57, 3.50)$; $H_{\text{Exp(ODEs,SSA)}}^{\text{plankton}} = 4.68(6.43, 6.48)$. Here the Shannon entropy $H = -\sum_{i=1}^{S_C} P_i \log_2(P_i)$, where P_i is the probability that a consumer individual belongs to species C_i .

Appendix references

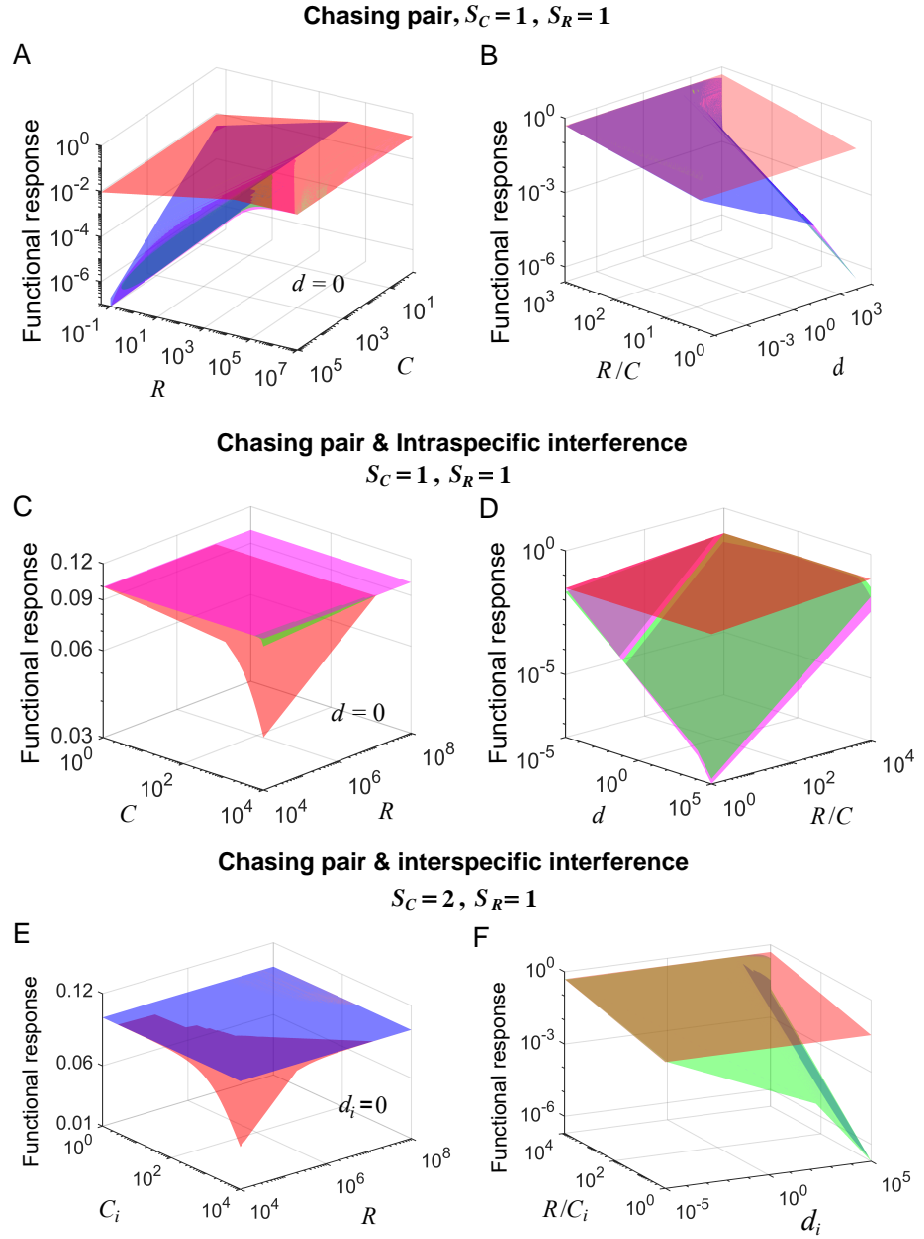
- Ayala FJ, Experimental invalidation of the principle of competitive exclusion. *Nature* **224**, 1076-1079 (1969).
- Beddington J R, Mutual interference between parasites or predators and its effect on searching efficiency. *J. Anim. Ecol.* **44**, 331-340 (1975).
- Clarke FM, Racey L, Life after logging: post-logging recovery of a neotropical bat community. *J. Appl. Ecol.* **42**, 409-420 (2005).
- Cody ML, Smallwood JA, *Long-Term Studies of Vertebrate Communities*. (Academic Press, 1996).
- DeAngelis DL, Goldstein RA, O'Neill RV, A model for trophic interaction. *Ecology* **56**, 881-892 (1975).
- Fuhrman JA et al., A latitudinal diversity gradient in planktonic marine bacteria. *Proc. Natl. Acad. Sci. U.S.A.* **105**, 7774-7778 (2008).
- Holmes RT, Sherry TW, Sturges FW, Bird Community Dynamics in a Temperate Deciduous Forest: Long-Term Trends at Hubbard Brook. *Ecol. Monogr.* **56**, 201-220 (1986).
- Hubbell SP, *The Unified Neutral Theory of Biodiversity and Biogeography*. (Princeton University Press, 2001).

- Huisman J, Weissing FJ, Biodiversity of plankton by species oscillations and chaos. *Nature* **402**, 407-410 (1999).
- Koch AL, Competitive coexistence of two predators utilizing the same prey under constant environmental conditions. *J. Theor. Biol.* **44**, 387-395 (1974).
- Levin SA, Community equilibria and stability, and an extension of the competitive exclusion principle. *Am. Nat.* **104**, 413-423 (1970).
- MacArthur R, Species packing and competitive equilibrium for many species. *Theor. Popul. Biol.* **1**, 1-11 (1970).
- MacArthur R, Levins R, Competition, habitat selection, and character displacement in a patchy environment. *Proc. Natl. Acad. Sci. U.S.A.* **51**, 1207-1210 (1964).
- Martínez AE *et al.*, The structure and organisation of an Amazonian bird community remains little changed after nearly four decades in Manu National Park. *Ecol. Lett.* **26**, 335-346 (2023).
- Menon P, Billen G, Servais P, Mortality rates of autochthonous and fecal bacteria in natural aquatic ecosystems. *Water Res.* **37**, 4151-4158 (2003).
- Park T, Experimental studies of interspecies competition ii. temperature, humidity, and competition in two species of tribolium. *Physiol. Zool.* **27**, 177-238 (1954).
- Ser-Giacomi E *et al.*, Ubiquitous abundance distribution of non-dominant plankton across the global ocean. *Nat. Ecol. Evol.* **2**, 1243-1249 (2018).
- Terborgh J, Robinson SK, Parker III TA, Munn CA, Pierpont N, Structure and organization of an amazonian forest bird community. *Ecol. Mono.* **60**, 213-238 (1990).
- Wang X, Liu YY, Overcome competitive exclusion in ecosystems. *iScience* **23**, 101009 (2020).

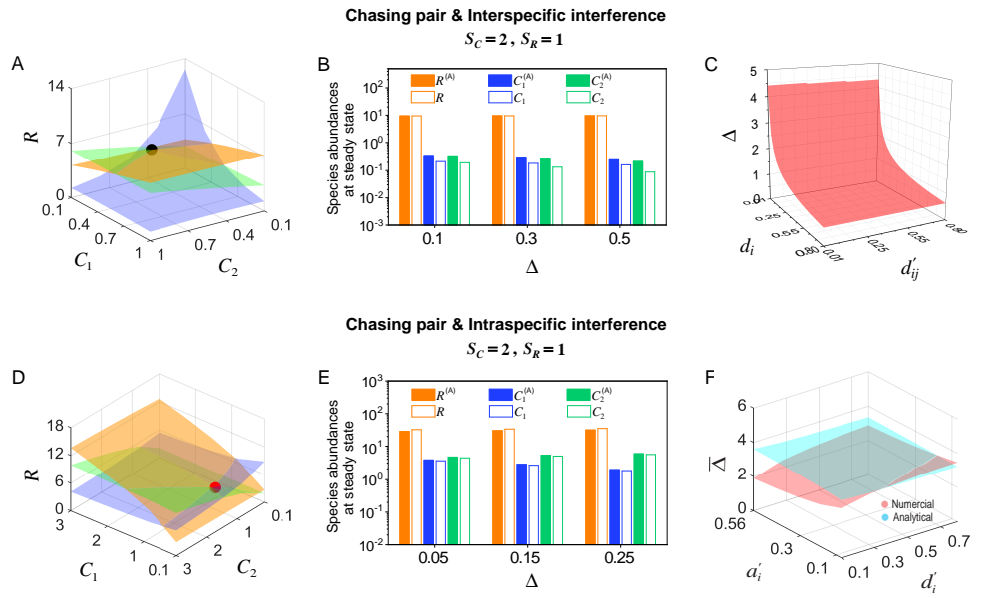
Appendix Figures



Appendix-figure 1. Estimation of the encounter rates with the mean-field approximations. To calculate a_{il} in the chasing pair, we suppose that all individuals of species R_l stand still while a C_i individual moves at the speed of $\overline{u_{C_i-R_l}}$ (the relative speed). Over a time interval of Δt , the length of zigzag trajectory of the C_i individual is approximately $\overline{u_{C_i-R_l}} \Delta t$, while the encounter area (marked with dashed lines) is estimated to be $2r_{il}^{(C)} \overline{u_{C_i-R_l}} \Delta t$. Then, we can estimate the encounter rate a_{il} using the encounter area and concentrations of the species (see Materials and Methods for details). Similarly, we can estimate a'_{ij} in the interference pair.



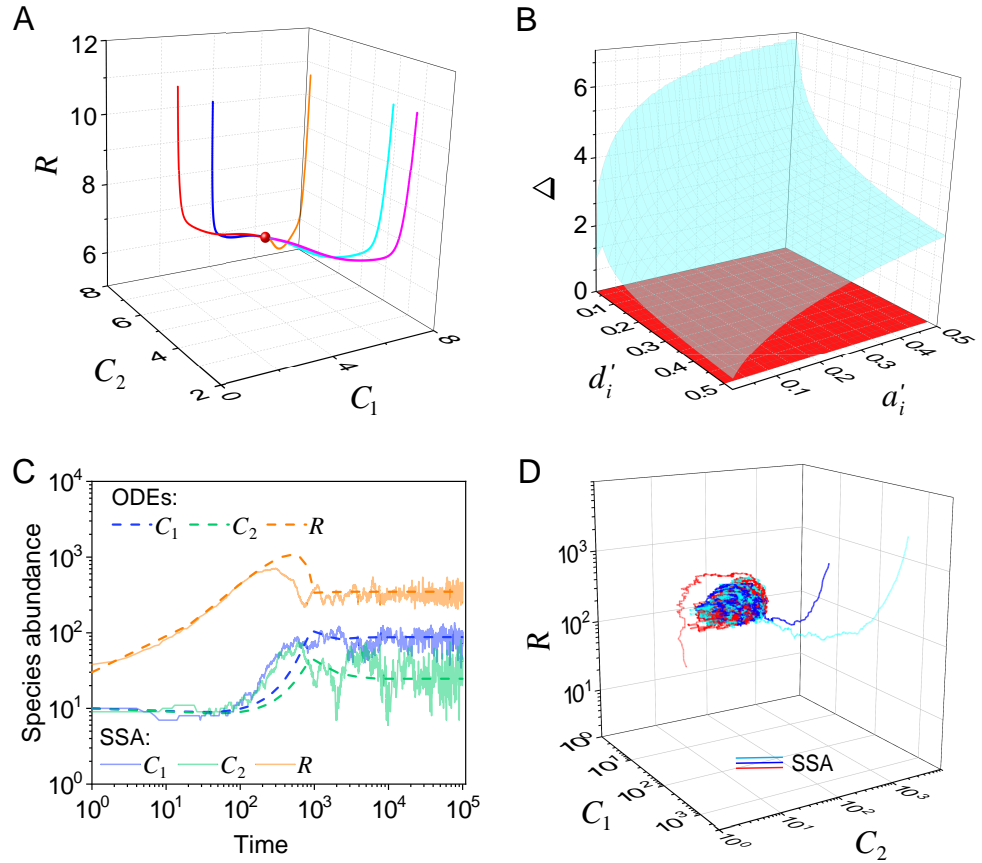
Appendix-figure 2. Functional response in scenarios involving different types of pairwise encounter. (A-B) In the scenario involving only chasing pair, the red surface corresponds to the B-D model (calculated from Eq.S10), while the green surface represents the exact solutions to our mechanistic model (calculated from Eq. S7). The magenta (calculated from Eq. S8) and blue (calculated from Eq. S9) surfaces represent the approximate solutions to our model. (C-D) In the scenario involving chasing pair and intraspecific interference, the red surface corresponds to the B-D model (calculated from Eq.S24), while the green surface represents the exact solutions to our mechanistic model (calculated from Eq. S17). The blue surface (calculated from Eq. S19) and the magenta surface (calculated from Eq. S21) represent the quasi-rigorous and the approximate solutions to our model, respectively. (E-F) In the scenario involving chasing pair and interspecific interference, the red surface corresponds to the B-D model (calculated from Eq. S31), while the green surface represents the quasi-rigorous solutions to our mechanistic model (calculated from Eq. S27). The blue surface (calculated from Eq. S29) represents the approximate solutions to our model. In (A-B): $k = 0.1, a = 0.25$. In (A): $d = 0$. (see Appendix II). In (C-D): $a = 0.1, k = 0.1, d' = 0.1, a' = 0.12$. In (C): $d = 0$ (see Appendix II). In (E-F): $a_1 = a_2 = 0.1, k_1 = k_2 = 0.1, d'_{12} = 0.1, a'_{12} = 0.12$. In (E): $d_i = 0$ ($i = 1, 2$) (see Appendix II).



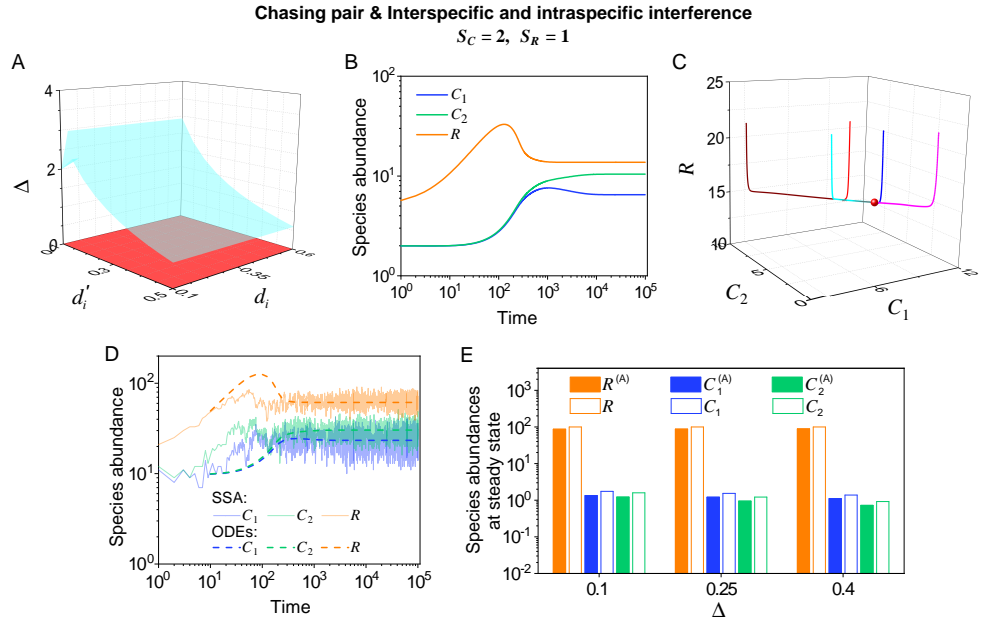
Appendix-figure 3. Fixed point solutions in scenarios involving chasing pair and different types of predator interference. Here, $S_C = 2$ and $S_R = 1$. D_i ($i = 1, 2$) is the only parameter varying with the consumer species (with $D_1 > D_2$), and $\Delta = (D_1 - D_2)/D_2$ represents the competitive difference between the two species. **(A-C)** Scenario involving chasing pair and interspecific interference. **(D-F)** Scenario involving chasing pair and intraspecific interference. **(A, D)** Positive solutions to the steady-state equations: $\hat{R} = 0$ (orange surface), $C_1 = 0$ (blue surface), $C_2 = 0$ (green surface). The intersection point marked by black/red dots is an unstable/stable fixed point. **(B, E)** Comparisons between the numerical results and analytical solutions of the species abundances at fixed points. Color bars are analytical solutions while hollow bars are numerical results. The analytical solutions in **(B)** and **(E)** (marked with superscript "A") were calculated from Eqs. S68, S70 and Eqs. S41, S43, respectively. **(C)** In this scenario, there is no parameter region for stable coexistence. The region below the red surface and above $\Delta = 0$ represents unstable fixed points. **(F)** Comparisons between the numerical results and analytical solutions of the coexistence region. Here $\bar{\Delta}$ represents the maximum competitive difference tolerated for species coexistence. The red and cyan surfaces represent the analytical solutions (calculated from Eq. S46) and numerical results, respectively. The numerical results in **(A-C)** and **(D-F)** were calculated from Eqs. S42, S61 and Eqs. S33, S42, respectively. In **(A)**: $a_1 = a_2 = 0.05$, $d_1 = d_2 = 0.05$, $K_0 = 20$, $a'_{12} = 0.06$, $d'_{12} = 0.01$, $k_1 = k_2 = 0.02$, $w_1 = w_2 = 0.08$, $D_1 = 0.0011$, $D_2 = 0.001$, $R_a = 0.01$. In **(B)**: $a_1 = a_2 = 0.04$, $d_1 = d_2 = 0.2$, $K_0 = 10$, $a'_{12} = 0.048$, $d'_{12} = 0.001$, $k_1 = k_2 = 0.1$, $w_1 = w_2 = 0.3$, $D_2 = 0.0008$, $R_a = 0.2$. In **(C)**: $a_1 = a_2 = 0.1$, $K_0 = 100$, $k_1 = k_2 = 0.1$, $w_1 = w_2 = 0.1$, $D_2 = 0.001$, $a'_{12} = 0.12$, $R_a = 0.05$. In **(D)**: $a_1 = a_2 = 0.5$, $a'_1 = a'_2 = 0.625$, $d_1 = d_2 = 0.5$, $d'_1 = d'_2 = 0.5$, $k_1 = k_2 = 0.4$, $D_2 = 0.02$, $w_1 = w_2 = 0.5$, $K_0 = 10$, $D_1 = 1.2D_2$, $R_a = 0.1$. In **(E)**: $a_1 = a_2 = 0.1$, $a'_1 = a'_2 = 0.12$, $k_1 = k_2 = 0.12$, $w_1 = w_2 = 0.3$, $D_2 = 0.02$, $K_0 = 100$, $R_a = 0.8$, $d_1 = d_2 = 0.5$, $d'_1 = d'_2 = 0.05$. In **(F)**: $a_1 = a_2 = 0.5$, $k_1 = k_2 = 0.2$, $w_1 = w_2 = 0.2$, $D_2 = 0.008$, $K_0 = 60$, $R_a = 0.8$, $d_1 = d_2 = 0.8$.

Chasing pair & Intraspecific interference

$$S_C = 2, S_R = 1$$

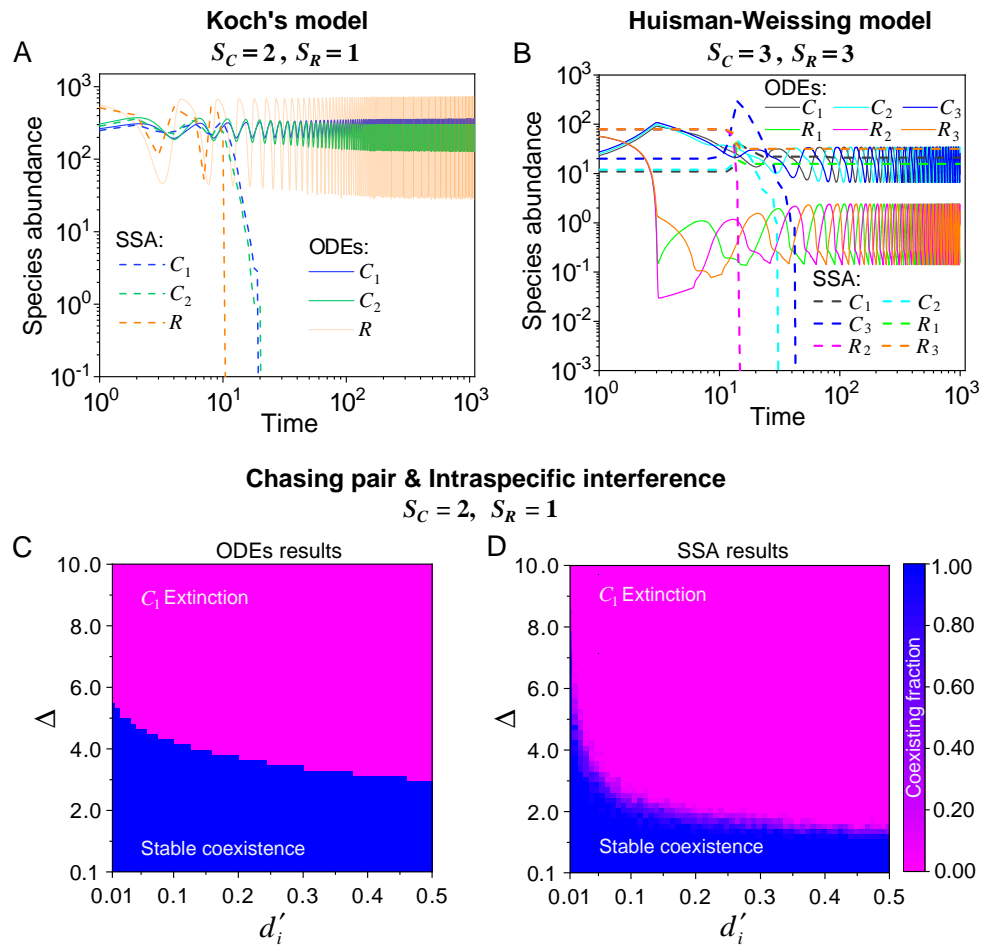


Appendix-figure 4. Intraspecific predator interference facilitates species coexistence regardless of stochasticity. Here we consider the case of $S_C = 2, S_R = 1$. **(A)** A representative trajectory of species coexistence in the phase space simulated with ODEs. The fixed point (shown in red) is stable and globally attractive. **(B)** A 3D phase diagram in the ODEs studies. D_i ($i = 1, 2$) is the only parameter that varies with the two consumer species, and $\Delta \equiv (D_1 - D_2)/D_2$ measures the competitive difference between the two species. The parameter region below the blue surface yet above the red surface represents stable coexistence. The region below the red surface and above $\Delta = 0$ represents unstable fixed points (an empty set). **(C)** Time courses of the species abundances simulated with ODEs or SSA. **(D)** Representative trajectories of species coexistence in the phase space simulated with SSA. The coexistence state is stable and globally attractive (see **(C)** for time courses, SSA results). **(A-D)** were calculated or simulated from Eqs. 1, 2, 4. In **(A)**: $a_i = 0.1, a'_i = 0.125, d_i = 0.1, d'_i = 0.05, w_i = 0.1, k_i = 0.1$ ($i = 1, 2$); $D_1 = 0.0035, D_2 = 0.0038, K_0 = 100, R_a = 0.3$. In **(B)**: $a_i = 0.1, d_i = 0.1, w_i = 0.1, k_i = 0.1$ ($i = 1, 2$); $K_0 = 100, D_2 = 0.001, \Delta = (D_1 - D_2)/D_2, K_0 = 100, R_a = 0.1$. In **(C-D)**: $a_i = 0.02, a'_i = 0.025, d_i = 0.7, d'_i = 0.7, w_i = 0.4, k_i = 0.05$ ($i = 1, 2$); $D_1 = 0.0160, D_2 = 0.0171, K_0 = 2000, R_a = 5.5$.



Appendix-figure 5. Outcomes of two consumers species competing for one resource species involving chasing pair and intra- and inter-specific interference. Here, D_i ($i = 1, 2$) is the only parameter that varies with the consumer species (with $D_1 > D_2$), and $\Delta = (D_1 - D_2)/D_2$ measures the competitive difference between the two species. **(A-C, E)** ODEs results. **(D)** ODEs and SSA results. **(A)** A 3D phase diagram. The parameter region below the blue surface yet above the red surface represents stable coexistence, while that below the red surface and above $\Delta = 0$ represents unstable fixed points (an empty set). **(B)** Time courses of the species abundances. Two consumer species may coexist with one type of resources at steady state. **(C)** Representative trajectories of species coexistence in the phase space. The fixed point (shown in red) is stable and globally attractive. **(D)** Consumer species may coexist indefinitely with the resources regardless of stochasticity. **(E)** Comparisons between numerical results and analytical solutions of the species abundances at fixed points. Color bars are analytical solutions while hollow bars are numerical results. The analytical solutions (marked with superscript "(A)") were calculated from Eqs. S74-S75. The numerical results in **(A-E)** were calculated or simulated from Eqs. 1-4. In **(A-C)**:

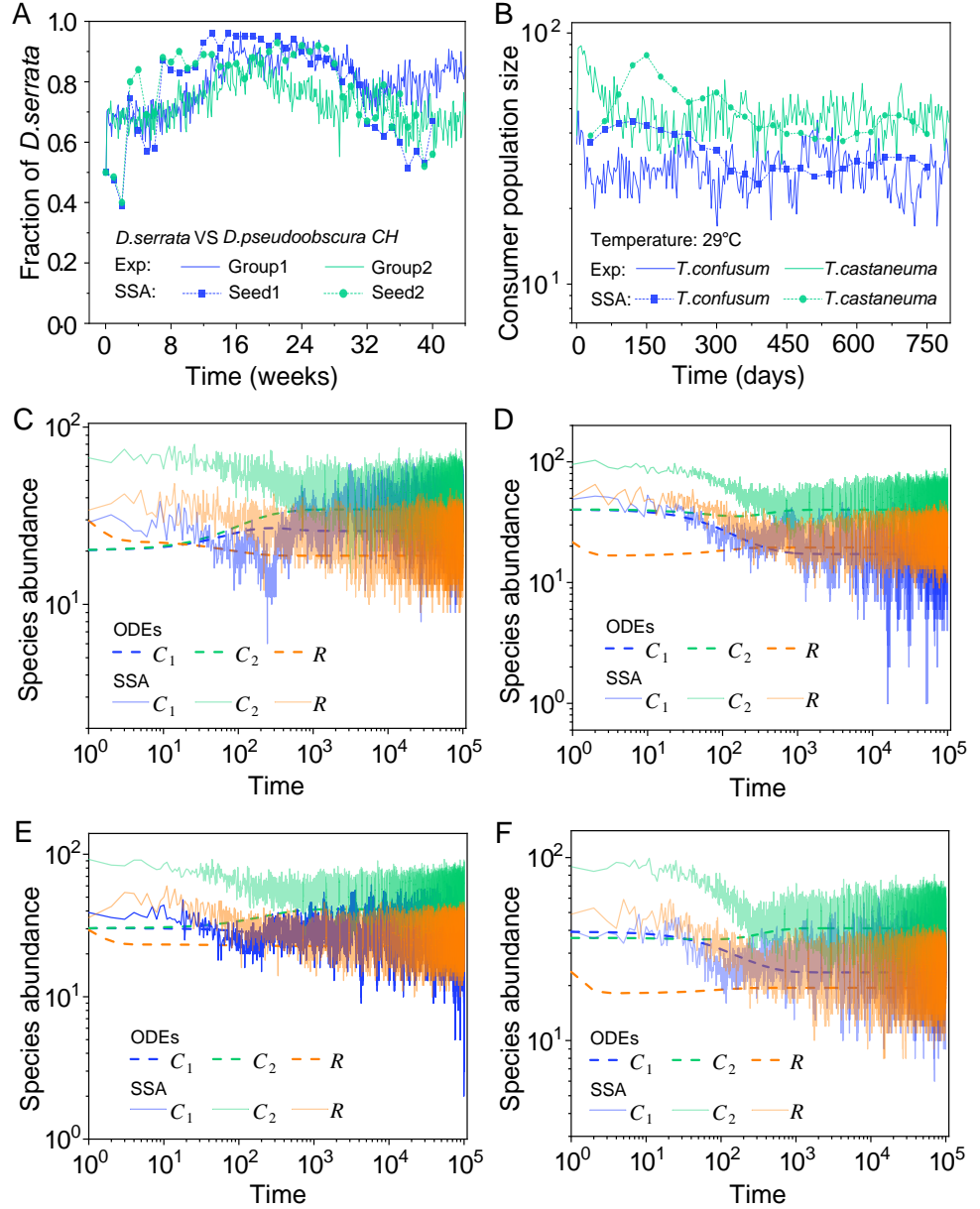
$a_1 = a_2 = 0.1, a'_1 = a'_2 = 0.12, k_1 = k_2 = 0.1, w_1 = w_2 = 0.1, D_2 = 0.004, K_0 = 100, a'_{12} = 0.12, R_a = 0.8, d'_{12} = 0.5$. In **(B-C)**: $d_1 = d_2 = 0.3, d'_1 = d'_2 = 0.5$. In **(D)**: $a_1 = a_2 = 0.1, a'_1 = a'_2 = 0.14, k_1 = k_2 = 0.12, w_1 = w_2 = 0.15, D_1 = 0.0125, D_2 = 0.012, K_0 = 300, R_a = 5.5, d_1 = d_2 = 0.3, d'_1 = d'_2 = 0.5, a'_{12} = 0.14, d'_{12} = 5$. In **(E)**: $a_1 = a_2 = 0.05, a'_1 = a'_2 = 0.06, k_1 = k_2 = 0.1, w_1 = w_2 = 0.2, D_2 = 0.008, K_0 = 100, R_a = 0.8, d_1 = d_2 = 0.5, d'_1 = d'_2 = 0.15, a'_{12} = 0.06, d'_{12} = 0.0005$.



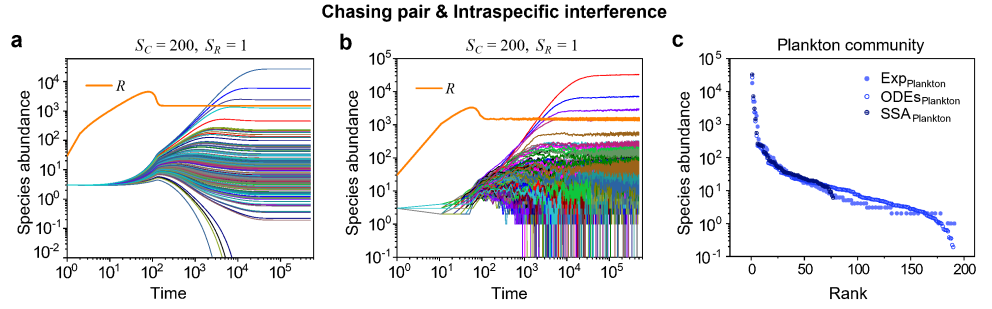
Appendix-figure 6. The influence of stochasticity on species coexistence. (A-B) Stochasticity jeopardizes species coexistence. Koch's model (Koch, 1974) and Huisman-Weissing model (Huisman and Weissing, 1999) were simulated with SSA using the same parameter settings as their deterministic model. Nevertheless, both cases of oscillating coexistence are vulnerable to stochasticity. See Ref. (Koch, 1974) and (Huisman and Weissing, 1999) for the parameters. (C-D) Phase diagrams in the scenario involving chasing pair and intraspecific interference. Here, $S_C = 2$ and $S_R = 1$. D_i ($i = 1, 2$) is the only parameter varying with the consumer species (with $D_1 > D_2$), and $\Delta = (D_1 - D_2)/D_2$ represents the competitive difference between the two species. (C) The ODEs results. (D) The SSA results (with the same parameter region as (C)). The species' coexisting fraction in each pixel was calculated from 16 random repeats. (C) and (D) were calculated from Eqs. 1, 2, 4. In (C-D): $a_i = 0.1, a'_i = 0.125, d_i = 0.5, w_i = 0.1, k_i = 0.1$ ($i = 1, 2$); $K_0 = 100, R_a = 5, D_2 = 0.0014$.

Chasing pair & Intraspecific interference

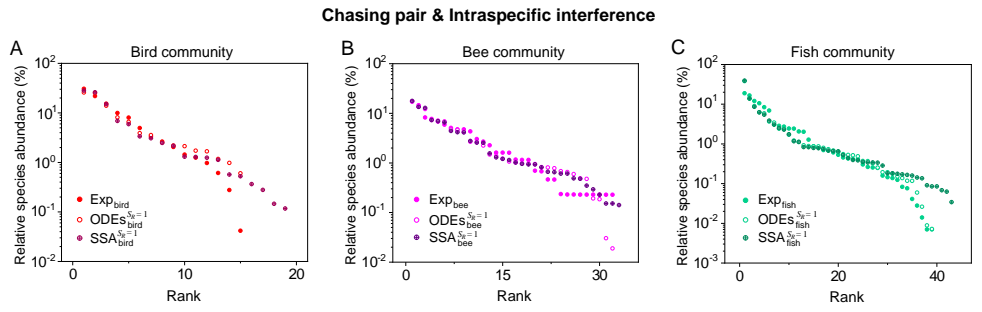
$$S_C = 2, S_R = 1$$



Appendix-figure 7. A model of intraspecific predator interference explains two classical experiments that invalidate CEP. **(A-B)** The solid icons represent the experimental data, which are connected by the dotted lines for the sake of visibility. The solid lines stand for the SSA simulation results. In all cases, two consumer species coexist for long with only one type of resources. **(A)** In Ayala's experiment (Ayala, 1969), two *Drosophila* species (consumers), *D. serrata* and *D. pseudoobscura*, compete for the same type of abiotic resources within a laboratory bottle. **(B)** In Park's experiment (Park, 1954), two *Tribolium* species, *T. confusum* and *T. castaneum*, compete for the same food (flour). **(C-F)** Time courses of the species abundances in the scenario involving chasing pair and intraspecific interference. The time series in **(C-F)** correspond to the long-term version of that shown in Fig. 2D, Appendix-fig. 7A, Fig. 2E, Appendix-fig. 7B, respectively. **(A-F)** were simulated from Eqs. 1, 2, 4. In **(A)**: $a_i = 0.3, a'_i = 0.33, w_i = 0.018, k_i = 4.8, d'_i = 5, d_i = 5.5$ ($i = 1, 2$); $D_2 = 0.010, R_a = 35, K_0 = 10000, D_1 = 0.0132$. In **(B)**: $w_i = 0.02, k_i = 4.5, d'_i = 4, d_i = 4.5$ ($i = 1, 2$); $D_2 = 0.010, R_a = 35, K_0 = 10000, a_i = 0.3, a'_i = 0.36$ ($i = 1, 2$); $D_1 = 0.0122$. In **(A-B)**: $\tau = 0.4$ Day (see).



Appendix-figure 8. A model of intraspecific interference semi-quantitatively illustrates the rank-abundance curve of a plankton community ($S_C \gg S_R$). (A-B) Intraspecific interference enables a wide range of consumers species to coexist with one type of resources. **(A)** Time courses of the species abundances simulated with ODEs. **(B)** Time series of the species abundances simulated with SSA (with the same as parameter settings as **(A)**). **(C)** The rank-abundance curve of a plankton community. The solid dots represent the experimental data (marked with “Exp”) reported in a recent study (*Ser-Giacomi et al., 2018*) (TARA_139.SUR.180.2000.DNA), while the hollow dots and those with “+” center are the ODEs and SSA results constructed from timestamp $t = 5.0 \times 10^5$ in the time series (see **(A)** and **(B)**), respectively. The Shannon entropies of the experimental data and simulation results for the plankton community are: $H_{\text{Exp(ODEs,SSA)}^{\text{Plankton}}} = 2.85(2.18, 2.00)$. In the model settings, $S_C = 200$ and $S_R = 1$. D_i ($i = 1, \dots, S_C$) is the only parameter that varies with the consumer species, which was randomly drawn from a Gaussian distribution $\mathcal{N}(\mu, \sigma)$. Here, μ and σ are the mean and standard deviation of the distribution. The numerical results in **(A-C)** were simulated from Eqs. 1, 2, 4. In **(A-C)**: $a_i = 0.1, a'_i = 0.125, d'_i = 0.5, d_i = 0.2, w_i = 0.2, k_i = 0.1, K_0 = 10^5, D_i = \mathcal{N}(1, 0.38) \times 0.008$ ($i = 1, \dots, 200$), $R_a = 150$.



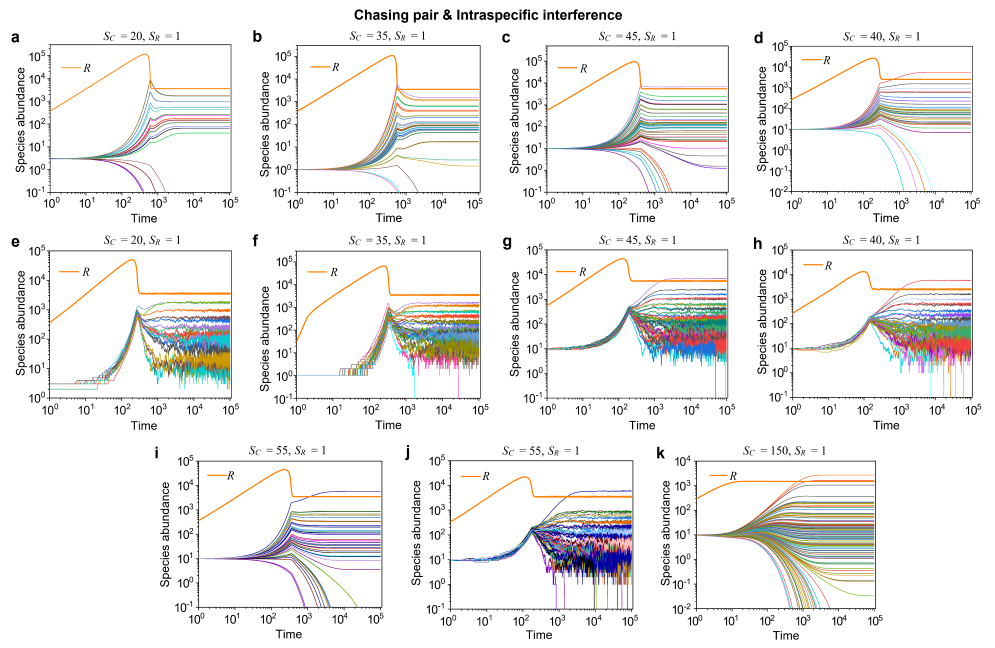
Appendix-figure 9. A model of intraspecific interference illustrates the rank-abundance curves across different ecological communities ($S_C \gg S_R$). The solid dots represent the experimental data (marked with “Exp”) reported in existing studies (Hubbell, 2001), (Holmes et al., 1986), (Cody et al., 1996), while the hollow dots and those with “+” center are the ODEs and SSA results constructed from timestamp $t = 1.0 \times 10^5$ in the time series (see Appendix-fig. 10A-G), respectively.

In the model settings, $S_R = 1$, $S_C = 20$ (in (A)), 35 (in (B)) or 45 (in (C)). D_i ($i = 1, \dots, S_C$) is the only parameter varying with the consumer species, which was randomly drawn from a Gaussian distribution. The Shannon entropies of the experimental data and simulation results for each ecological community are: $H_{\text{Exp}(\text{ODEs,SSA})}^{\text{bird}} = 2.98(3.06, 2.98)$, $H_{\text{Exp}(\text{ODEs,SSA})}^{\text{bee}} = 4.04(4.02, 4.02)$,

$H_{\text{Exp}(\text{ODEs,SSA})}^{\text{fish}} = 3.78(3.40, 3.41)$. In the Kolmogorov-Smirnov (K-S) test, the probabilities (p values) that the simulation results and the corresponding experimental data come from identical distributions are:

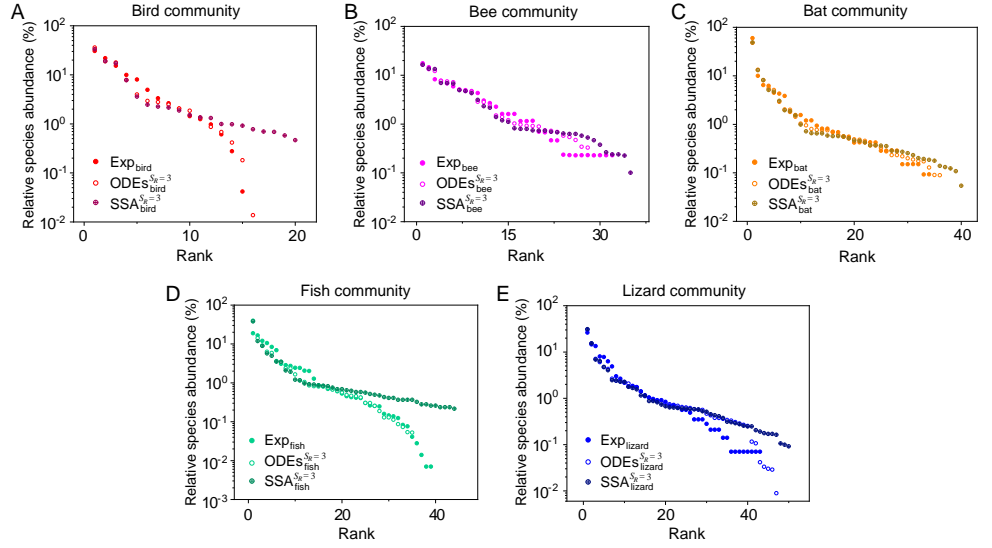
$p_{\text{ODEs}}^{\text{bird}} = 0.89$, $p_{\text{SSA}}^{\text{bird}} = 0.88$; $p_{\text{ODEs}}^{\text{bee}} = 0.47$, $p_{\text{SSA}}^{\text{bee}} = 0.75$; $p_{\text{ODEs}}^{\text{fish}} = 0.88$, $p_{\text{SSA}}^{\text{fish}} = 0.77$. With a significance threshold of 0.05, none of the p values suggest there exists a statistically significant difference. The numerical results in (A-C) were simulated from Eqs. 1, 2, 4. In (A):

$a_i = 0.1$, $a'_i = 0.125$, $d_i = 0.5$, $d'_i = 0.6$, $w_i = 0.22$, $k_i = 0.1$, $D_i = 0.016 \times \mathcal{N}(1, 0.35)$ ($i = 1, \dots, 20$); $R_a = 350$, $K_0 = 10^6$. In (B): $a_i = 0.1$, $a'_i = 0.125$, $d_i = 0.5$, $d'_i = 0.6$, $w_i = 0.22$, $k_i = 0.1$, $D_i = 0.012 \times \mathcal{N}(1, 0.35)$ ($i = 1, \dots, 35$); $R_a = 350$, $K_0 = 10^6$. In (C): $a_i = 0.1$, $a'_i = 0.14$, $d_i = 0.5$, $d'_i = 0.5$, $w_i = 0.2$, $k_i = 0.1$, $D_i = 0.015 \times \mathcal{N}(1, 0.32)$ ($i = 1, \dots, 45$); $R_a = 550$, $K_0 = 10^6$.

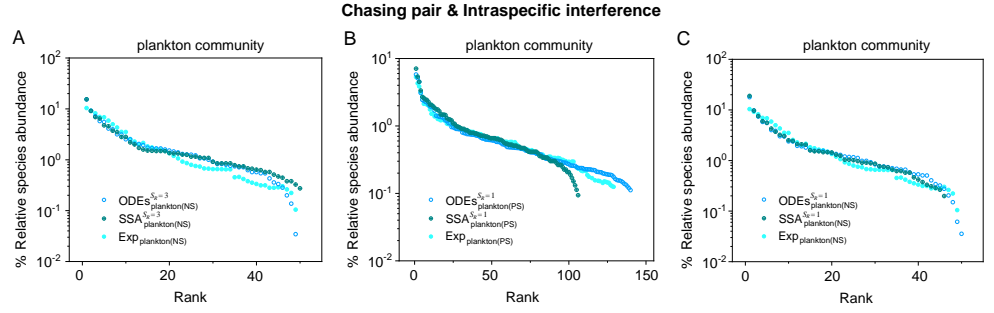


Appendix-figure 10. Time courses of the species abundances in the scenario involving chasing pair and intraspecific interference. The time series in (A, E), (B, F), (C, G), (D, H), (I, J) and (K) correspond to that shown in Appendix-fig. 9A-C, Fig. 3D (bat), Fig. 3D (lizard) and Fig. 3C (butterfly), respectively.

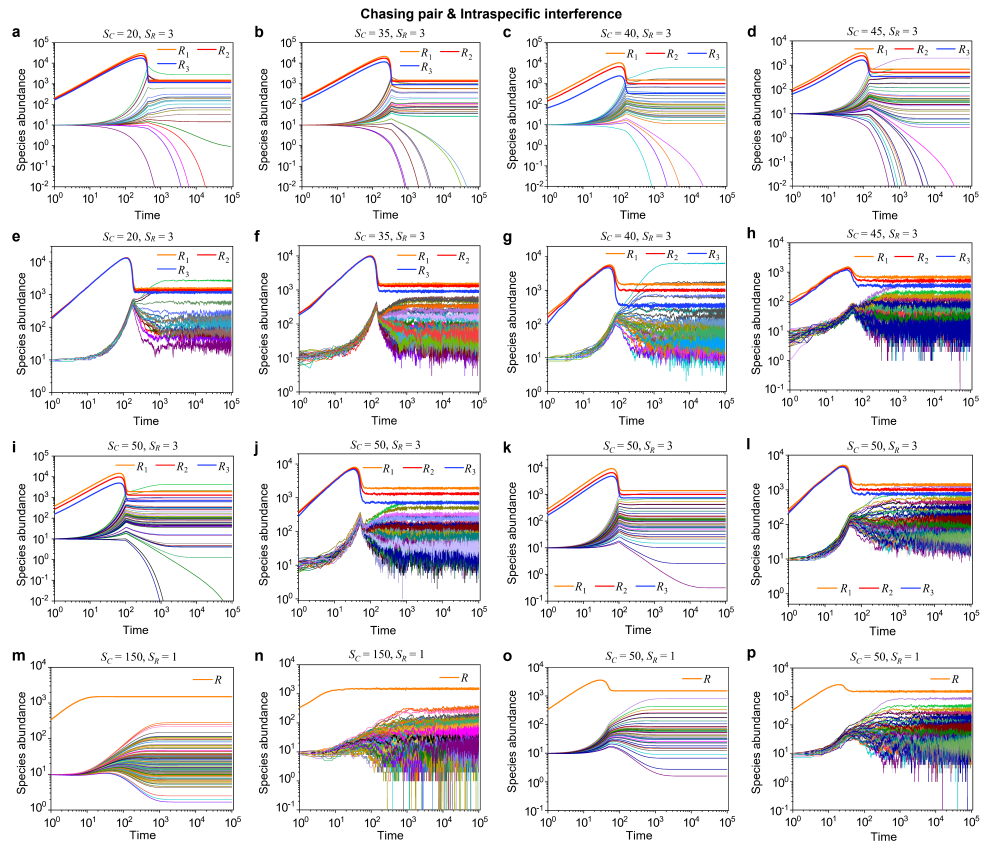
Chasing pair & Intraspecific interference



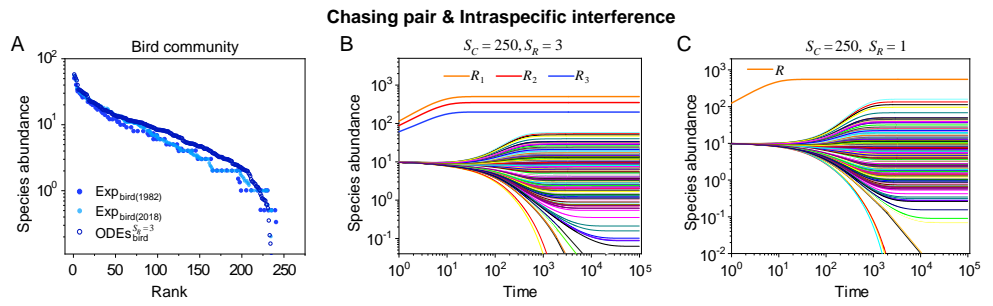
Appendix-figure 11. A model of intraspecific interference illustrates the rank-abundance curves across different ecological communities ($S_C \gg S_R$). The solid dots represent the experimental data (marked with “Exp”) reported in existing studies (Hubbell, 2001), (Holmes et al., 1986), (Cody et al., 1996), (Clarke et al., 2005), while the hollow dots and those with “+” center are the ODEs and SSA results constructed from timestamp $t = 1.0 \times 10^5$ in the time series (see Appendix-fig. 13), respectively. In the model settings, $S_R = 3$, $S_C = 20$ (in (A)), 35 (in (B)), 40 (in (C)), 45 (in (D)) or 50 (in (E)). D_i ($i = 1, \dots, S_C$) is the only parameter varying with the consumer species, which was randomly drawn from each ecological community are: $H_{\text{Exp(ODEs,SSA)}}^{\text{Bird}} = 2.98(2.98, 3.26)$, $H_{\text{Exp(ODEs,SSA)}}^{\text{Bee}} = 4.04(4.34, 4.35)$, $H_{\text{Exp(ODEs,SSA)}}^{\text{Bat}} = 3.00(3.00, 3.00)$, $H_{\text{Exp(ODEs,SSA)}}^{\text{Fish}} = 3.78(3.28, 3.64)$, $H_{\text{Exp(ODEs,SSA)}}^{\text{Lizard}} = 4.05(3.94, 3.94)$. In the K-S test, the p values that the simulation results and the corresponding experimental data come from identical distributions are: $p_{\text{ODEs}}^{\text{Bird}} = 0.59$, $p_{\text{SSA}}^{\text{Bird}} = 0.43$, $p_{\text{ODEs}}^{\text{Bee}} = 0.47$, $p_{\text{SSA}}^{\text{Bee}} = 0.33$, $p_{\text{ODEs}}^{\text{Bat}} = 0.42$, $p_{\text{SSA}}^{\text{Bat}} = 0.27$, $p_{\text{ODEs}}^{\text{Fish}} = 0.22$, $p_{\text{SSA}}^{\text{Fish}} = 0.06$, $p_{\text{ODEs}}^{\text{Lizard}} = 0.56$, $p_{\text{SSA}}^{\text{Lizard}} = 0.36$. With a significance threshold of 0.05, none of the p values suggest there exists a statistically significant difference. The numerical results in (A-E) were simulated from Eqs. 1, 2, 4. In (A-E): $a_{il} = 0.1$, $a'_i = 0.125$, $d_{il} = 0.5$. In (A): $d'_i = 0.3$, $w_{il} = 0.2$, $k_{il} = 0.12$, $K_0^{(1)} = 8 \times 10^4$, $K_0^{(2)} = 5 \times 10^4$, $K_0^{(3)} = 3 \times 10^4$, $D_i = 0.021 \times \mathcal{N}(1, 0.28)$ ($i = 1, \dots, 20, l = 1, 2, 3$); $R_a^{(1)} = 180$, $R_a^{(2)} = 160$, $R_a^{(3)} = 140$. In (B): $d'_i = 0.6$, $w_{il} = 0.2$, $k_{il} = 0.12$, $K_0^{(1)} = 8 \times 10^4$, $K_0^{(2)} = 5 \times 10^4$, $K_0^{(3)} = 3 \times 10^4$, $D_i = 0.017 \times \mathcal{N}(1, 0.3)$ ($i = 1, \dots, 35, l = 1, 2, 3$); $R_a^{(1)} = 180$, $R_a^{(2)} = 160$, $R_a^{(3)} = 110$. In (C): $d'_i = 0.4$, $w_{il} = 0.3$, $k_{il} = 0.12$, $K_0^{(1)} = 10^5$, $K_0^{(2)} = 5 \times 10^4$, $K_0^{(3)} = 3 \times 10^4$, $D_i = 0.023 \times \mathcal{N}(1, 0.34)$ ($i = 1, \dots, 40, l = 1, 2, 3$); $R_a^{(1)} = 180$, $R_a^{(2)} = 120$, $R_a^{(3)} = 40$. In (D): $d'_i = 0.3$, $w_{il} = 0.3$, $k_{il} = 0.12$, $K_0^{(1)} = 8 \times 10^4$, $K_0^{(2)} = 5 \times 10^4$, $K_0^{(3)} = 3 \times 10^4$, $D_i = 0.027 \times \mathcal{N}(1, 0.32)$ ($i = 1, \dots, 45, l = 1, 2, 3$); $R_a^{(1)} = 80$, $R_a^{(2)} = 60$, $R_a^{(3)} = 40$. In (E): $d'_i = 0.3$, $w_{il} = 0.3$, $k_{il} = 0.2$, $K_0^{(1)} = 3 \times 10^5$, $K_0^{(2)} = 10^5$, $K_0^{(3)} = 3 \times 10^4$, $D_i = 0.034 \times \mathcal{N}(1, 0.34)$ ($i = 1, \dots, 50, l = 1, 2, 3$); $R_a^{(1)} = 380$, $R_a^{(2)} = 260$, $R_a^{(3)} = 140$.



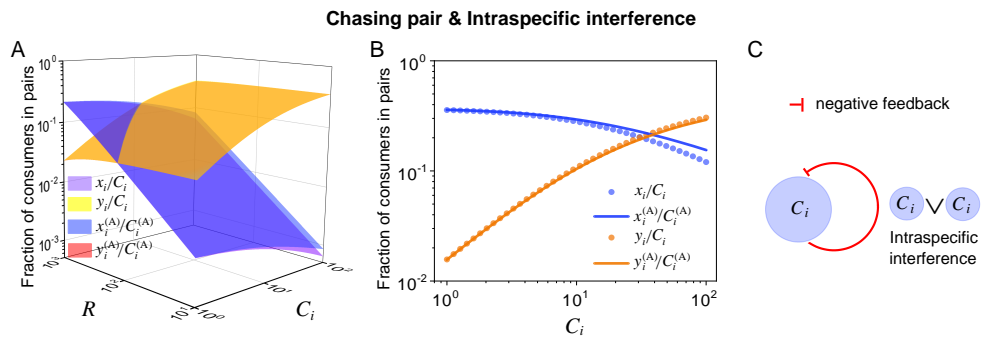
Appendix-figure 12. A model of intraspecific interference illustrates the rank-abundance curves across different plankton communities ($S_C \gg S_R$). The solid dots represent the experimental data (marked with “Exp”) reported in a recent study (Fuhrman *et al.*, 2008), while the hollow dots and those with “+” center are the ODEs and SSA results constructed from timestamp $t = 1.0 \times 10^5$ in the time series (see Appendix-fig. 13), respectively. The plankton community data were obtained separately from the Norwegian Sea (NS) and Pacific Station (PS). In the model settings, $S_R = 1$ (in (B-C)), 3 (in (A)); $S_C = 50$ (in (A, C)), 150 (in (B)). D_i ($i = 1, \dots, S_C$) is the only parameter varying with the consumer species, which was randomly drawn from a Gaussian distribution. The Shannon entropies of the experimental data and simulation results for each plankton community are: $H_{\text{Exp(ODEs,SSA)}}^{\text{plankton(NS)}} = 4.67(4.85, 4.90)$ for $S_R = 3$; $H_{\text{Exp(ODEs,SSA)}}^{\text{plankton(PS)}} = 4.68(6.53, 6.16)$, $H_{\text{Exp(ODEs,SSA)}}^{\text{plankton(NS)}} = 4.67(4.74, 4.64)$ for $S_R = 1$. In the K-S test, the p values that the simulation results and the corresponding experimental data come from identical distributions are: $p_{\text{ODEs}}^{\text{plankton(NS)}} = 0.31$, $p_{\text{SSA}}^{\text{plankton(NS)}} = 0.14$ for $S_R = 3$; $p_{\text{ODEs}}^{\text{plankton(PS)}} = 0.08$; $p_{\text{SSA}}^{\text{plankton(PS)}} = 0.28$, $p_{\text{ODEs}}^{\text{plankton(NS)}} = 0.46$, $p_{\text{SSA}}^{\text{plankton(NS)}} = 0.37$ for $S_R = 1$. With a significance threshold of 0.05, none of the p values suggest there exists a statistically significant difference. The numerical results in (A-C) were simulated from Eqs. 1, 2, 4. In (A): $a_{il} = 0.1$, $a'_i = 0.125$, $d_{il} = 0.5$, $d'_i = 0.2$, $w_{il} = 0.3$, $k_{il} = 0.2$, $K_0^{(1)} = 8 \times 10^4$, $K_0^{(2)} = 5 \times 10^4$, $K_0^{(3)} = 3 \times 10^4$, $R_a^{(1)} = 280$, $R_a^{(2)} = 200$, $R_a^{(3)} = 150$, $D_i = 0.035 \times \mathcal{N}(1, 0.25)$ ($i = 1, \dots, 50$, $l = 1, 2, 3$). In (B): $a_i = 0.1$, $a'_i = 0.125$, $d_i = 0.3$, $d'_i = 0.3$, $w_i = 0.3$, $k_i = 0.2$, $D_i = 0.025 \times \mathcal{N}(1, 0.25)$ ($i = 1, \dots, 150$, $l = 1, 2, 3$); $R_a = 350$, $K_0 = 10^4$. In (C): $a_i = 0.1$, $a'_i = 0.125$, $d_i = 0.3$, $d'_i = 0.3$, $w_i = 0.3$, $k_i = 0.2$, $R_a = 350$, $K_0 = 10^4$, $D_i = 0.03 \times \mathcal{N}(1, 0.27)$ ($i = 1, \dots, S_C$).



Appendix-figure 13. Time courses of the species abundances in the scenario involving chasing pair and intraspecific interference. The time series in (A, E), (B, F), (C, G), (D, H), (I, J), (K, L), (M, N) and (O, P) correspond to that shown in Appendix-figs. 11A-E and 12A-C, respectively.



Appendix-figure 14. A model of intraspecific interference illustrates the rank-abundance curve of a bird community ($S_C \gg S_R$). (A) The rank-abundance curve. The solid dots represent the bird community data (marked with "Exp") collected longitudinally within the same Amazonian region in 1982 (blue) and 2018 (cyan) (Terborgh *et al.*, 1990), (Martínez *et al.*, 2023). The hollow dots are the ODEs results constructed from timestamp $t = 1.0 \times 10^5$ in the time series (see (B)). (B) Time courses of the species abundances simulated with ODEs. In the model settings, $S_R = 3$ and $S_C = 250$. D_i ($i = 1, \dots, S_C$) is the only parameter varying with the consumer species, which was randomly drawn from a Gaussian distribution. The Shannon entropies of the experimental data and simulation results for the bird community are $H_{\text{Exp(ODEs)}}^{\text{bird(1982/2018)}} = 5.67/6.63(7.31)$. In the K-S test, the p values that the simulation results and the corresponding experimental data come from identical distributions are: $p_{\text{ODEs}}^{\text{bird(1982)}} = 0.28$, $p_{\text{ODEs}}^{\text{bird(2018)}} = 0.46$. With a significance threshold of 0.05, none of the p values suggest there exists a statistically significant difference. (C) Time courses of the species abundances simulated with ODEs corresponding to Fig. 3A (bird), and the simulation parameters are the same as Fig. 3A (bird). The numerical results in (A-C) were simulated from Eqs. 1, 2, 4. In (A-B): $a_{il} = 0.1$, $a'_i = 0.125$, $d_{il} = 0.5$, $d'_i = 0.6$, $w_{il} = 0.3$, $k_{il} = 0.2$, $D_i = 0.032 \times \mathcal{N}(1, 0.17)$ ($i = 1, \dots, 250, l = 1, 2, 3$); $K_0^{(1)} = 5 \times 10^4$, $K_0^{(2)} = 3 \times 10^4$, $K_0^{(3)} = 10^4$, $R_a^{(1)} = 100$, $R_a^{(2)} = 70$, $R_a^{(3)} = 40$.



Appendix-figure 15. Intraspecific interference results in an underlying negative feedback loop and thus promotes biodiversity. (A-B) The fraction of consumer individuals engaged in pairwise encounter. Here, $S_C = 40$ and $S_R = 1$. x_i represents $C_i^{(P)} \vee R^{(P)}$, and y_i represents $C_i^{(P)} \vee C_i^{(P)}$. x_i/C_i and y_i/C_i stand for the fractions of consumer individuals within a chasing pair and an interference pair, respectively. The numerical results were calculated from Eq. S55, while the analytical solutions (marked with superscript "(A)") were calculated from Eq. S59. The orange surface in (A) is an overlap of the red and yellow surfaces. (C) The formation of intraspecific interference results in a self-inhibiting negative feedback loop. In (A-B): $a_i = 0.0015$, $a'_i = 0.0021$, $d_i = 0.1$, $d'_i = 0.05$, $k_i = 5$. In (B): $R = 2000$.